Kupffer cells. Two authors counted the number of Kupffer cells in three separate 0.25-mm^2 areas within each specimen from both the nodular lesion and the nonnodular adjacent tissue. The mean values of the three cell counts were used for calculations. The Kupffer cell ratio was calculated using the following formula: mean Kupffer cell count of nodular lesion / mean Kupffer cell count of nonnodular adjacent tissue.

Therefore, the Kupffer cell ratio was less than 1 when fewer Kupffer cells were in the nodular lesion than in the nonnodular adjacent tissue, whereas the Kupffer cell ratio was greater than 1 when more Kupffer cells were in the nodular lesion than in the nonnodular adjacent tissue.

Statistical Analysis

The Kruskal-Wallis test, Mann-Whitney *U* test with Bonferroni inequality, and chi-square test were used to confirm the differences between the groups. The level of significance was set at $p < 0.05$ (m × n chi-square test, Mann-Whitney *U* test, and chi-square test). All analyses were performed with statistics software (SPSS, version 11, SPSS) for Microsoft Windows.

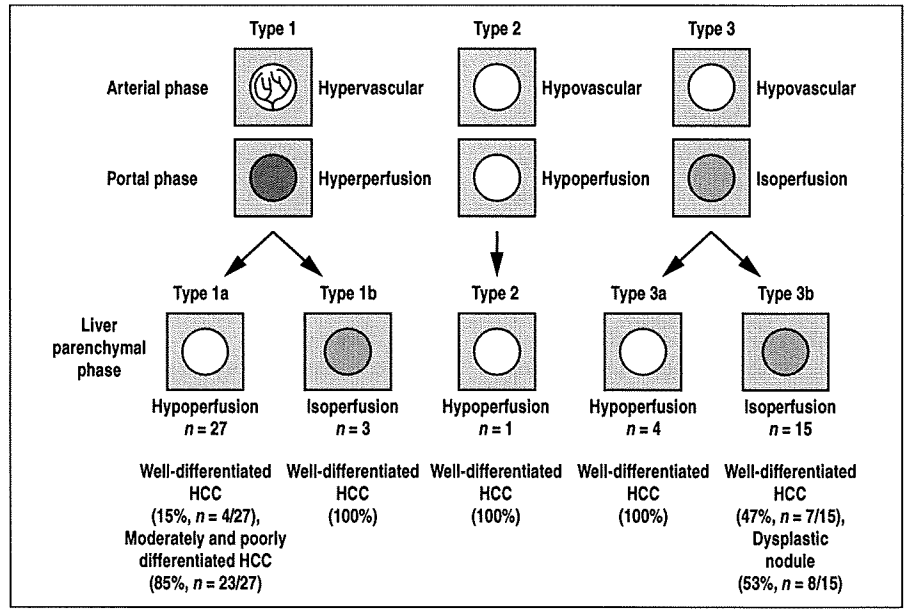

Fig. 1—Diagram shows perfusion patterns in hepatocellular carcinomas (HCCs) and dysplastic nodules on vascular and liver parenchymal phase imaging. Evaluation of vascular phase imaging allows tumors to be classified according to morphologic characteristics into type 1 nodules (moderately and poorly differentiated HCCs) and type 3 nodules (dysplastic nodules). With addition of liver parenchymal phase imaging, it is possible to subdivide type 1 and type 3 nodules further into type 1a, type 1b, type 3a, and type 3b, respectively. Well-differentiated HCCs exhibit various intranodular hemodynamic patterns.

Results

The 50 nodules were sorted into groups according to morphology: dysplastic nodules, $n = 8$; well-differentiated HCCs, $n = 19$; moderately differentiated HCCs, $n = 22$; and poorly differentiated HCC, $n = 1$. Moderately differentiated and poorly differentiated HCCs were merged to form one group (moderately and poorly differentiated HCC group), yielding a total of three groups that were used in the subsequent analyses. The median diameter of the tumors was 2.7 cm (range, 1.2–5.2 cm) as determined by sonography.

Intranodular Hemodynamic Patterns on Contrast-Enhanced Sonography

The arterial, portal phase, and liver parenchymal imaging perfusion patterns for each tumor analyzed using contrast-enhanced sonography were classified as shown in Figure 1. In the type 1 group, 27 tumors, four well-differentiated HCCs and 23 moderately and poorly differentiated HCCs, were classified as type 1a. The three well-differentiated HCCs were classified as type 1b. The type 2 tumor showed hypoperfusion in the liver parenchymal phase. Four well-differentiated HCCs were classified as type 3a. Seven well-differentiated HCCs and eight dysplastic nodules were classified as type 3b. In the liver parenchymal phase, all eight dysplastic nodules showed homogeneous isoperfusion relative to the adjacent liver. Ten (53%) well-differentiated HCCs showed homogeneous isoperfusion relative to adjacent liver, whereas nine (47%) well-differentiated HCCs showed perfusion defects. All 23 moderately and poorly differentiated HCCs showed a hypoperfusion pattern in the liver parenchymal phase. The number of tumors that showed isovascular staining in the liver parenchymal phase decreased as the nodules became less differentiated ($p < 0.05$, m × n chi-square test).

After we classified the perfusion patterns of the tumors during the arterial and portal phases and the liver parenchymal phase, we calculated the sensitivity, specificity, and accuracy of the diagnostic methods that use arterial and portal phase imaging only and of those that use a combination of arterial and portal phase imaging with liver parenchymal

TABLE 1: Diagnostic Accuracy of Two Imaging Methods for Histologic Grade of Hepatocellular Carcinoma (HCC)

Diagnosis	Vascular Phase Imaging Alone			Vascular Phase and Liver Parenchymal Phase Imaging		
	Sensitivity (%)	Specificity (%)	Accuracy (%)	Sensitivity (%)	Specificity (%)	Accuracy (%)
Moderately and poorly differentiated HCCs ($n = 23$)						
Type 1	100 (23/23)	74 (20/27)	86 (43/50)			
Type 1a				100 (23/23)	85 (23/27)	92 (46/50)
Dysplastic nodules ($n = 8$)						
Type 3	100 (8/8)	74 (31/42)	78 (39/50)			
Type 3b				100 (8/8)	83 (35/42)	86 (43/50)

Note—There were 19 well-differentiated HCCs. Data in parentheses are number of cases diagnosed / total number of cases.

phase imaging (Table 1). First, arterial and portal phase findings were used to calculate these three values. When type 1 was defined as the typical pattern for moderately and poorly differentiated HCC, sensitivity, specificity, and accuracy were 100%, 74%, and 86%, respectively. When type 3 was defined as a dysplastic nodule, the sensitivity, specificity, and accuracy were 100%, 74%, and 78%, respectively. Well-differentiated HCCs exhibited various intranodular hemodynamic patterns on arterial and portal phase imaging; we did not calculate these values. Second, a combination of arterial and portal phase imaging with liver parenchymal phase imaging was used to calculate sensitivity, specificity, and accuracy.

When type 1a was defined as the typical pattern for moderately and poorly differentiated HCC, the sensitivity, specificity, and accuracy were 100%, 85%, and 92%, respectively. When type 3b was defined as a dysplastic nodule, the sensitivity, specificity, and accuracy were 100%, 83%, and 86%, respectively. The diagnostic accuracy of contrast-enhanced sonography for dysplastic nodules showed a trend for improvement with the addition of liver parenchymal phase imaging (p = 0.07, chi-square test). Similar to arterial and portal phase imaging, liver parenchymal phase imaging showed that well-differentiated HCCs exhibit various intranodular hemodynamic patterns, so we did not calculate these values. However, using liver parenchymal phase imaging, we were able to diagnose seven nodules as type 3a and type 1b well-differentiated HCCs. Diagnosis of these seven nodules was not possible using arterial and portal phase imaging only.

After completion of this study, all type 1, type 2, two type 3a, and three type 3b well-differentiated HCCs were treated. All dysplastic nodules, two type 3a nodules, and four type 3b well-differentiated HCCs were followed up without treatment. Two patients were not treated because their liver function was Child-Pugh C and their ascites did not respond to diuretics. The intranodular hemodynamics of all the dysplastic nodules and of type 3b well-differentiated HCCs did not change in terms of size and vascularity during the 2-year follow-up period (Fig. 2). However, during the 1-year follow-up period, both untreated cases of type 3a well-differentiated HCC had progressed to overt hypervascular HCC on contrast-enhanced CT (Fig. 3).

Quantitative Analysis of Kupffer Cell Count

We compared the Kupffer cell ratios of tumors between groups that were classified according to perfusion patterns in the liver parenchymal phase. Kupffer cell ratios of tumors that showed hypoperfusion in the liver parenchymal phase were significantly lower than those of tumors that showed isoperfusion ($p < 0.05$, Mann-Whitney U test) (Fig. 4).

Discussion

Albrecht et al. [9] mentioned that Levovist is taken up by Kupffer cells, thereby providing specific liver enhancement. This characteristic of Levovist is considered to make it an echo source during liver parenchymal phase imaging. Therefore, liver parenchymal phase imaging might show different findings according to the number of Kupffer cells detected, allowing determination of the histologic grade of the tumor. The main purpose of this study was to investigate the possibility

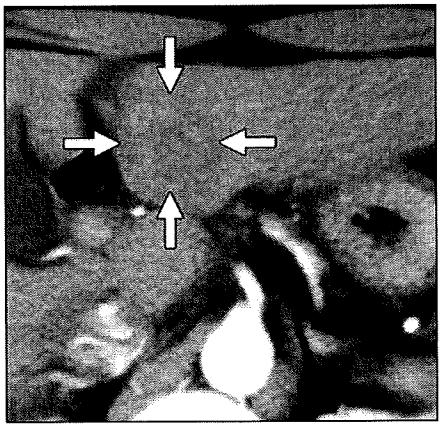

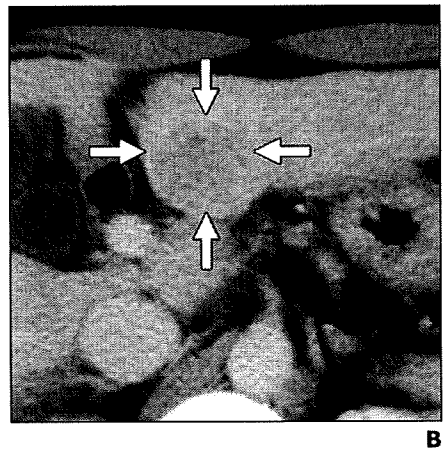

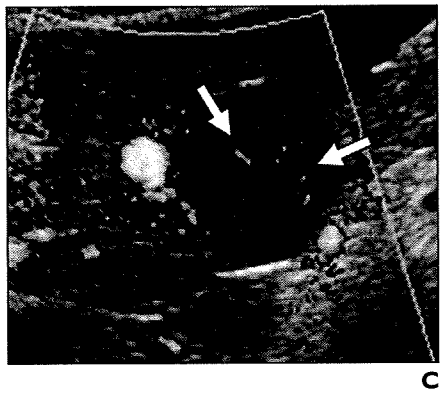

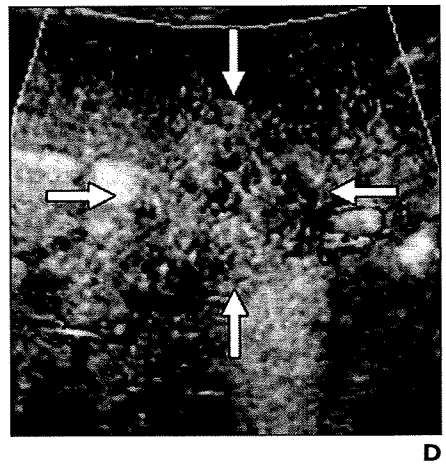

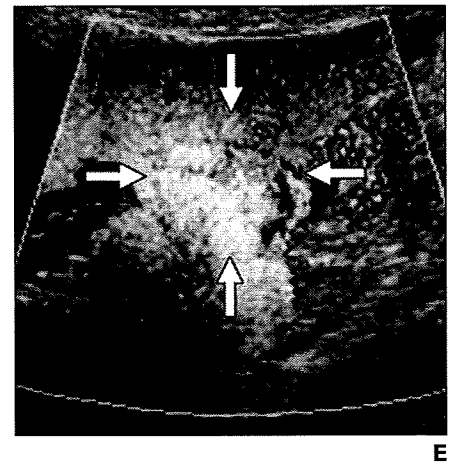

Fig. 2—Case presentation of 61-year-old man with well-differentiated hepatocellular carcinoma.
A and **B**, Hypoattenuation of nodule (*arrows*) is shown on arterial phase (**A**) and portal phase (**B**) dynamic CT scans.
C, Contrast-enhanced wideband color Doppler image shows a few internal blood vessels in tumor (*arrows*) during arterial phase.
D, Perfusion imaging of contrast-enhanced wideband color Doppler image shows tumor parenchymal staining as isoechoic (*arrows*) in portal phase.
E, Isoechoic tumor parenchymal staining (*arrows*) is shown in liver parenchymal phase.
(Fig. 2 continues on next page)

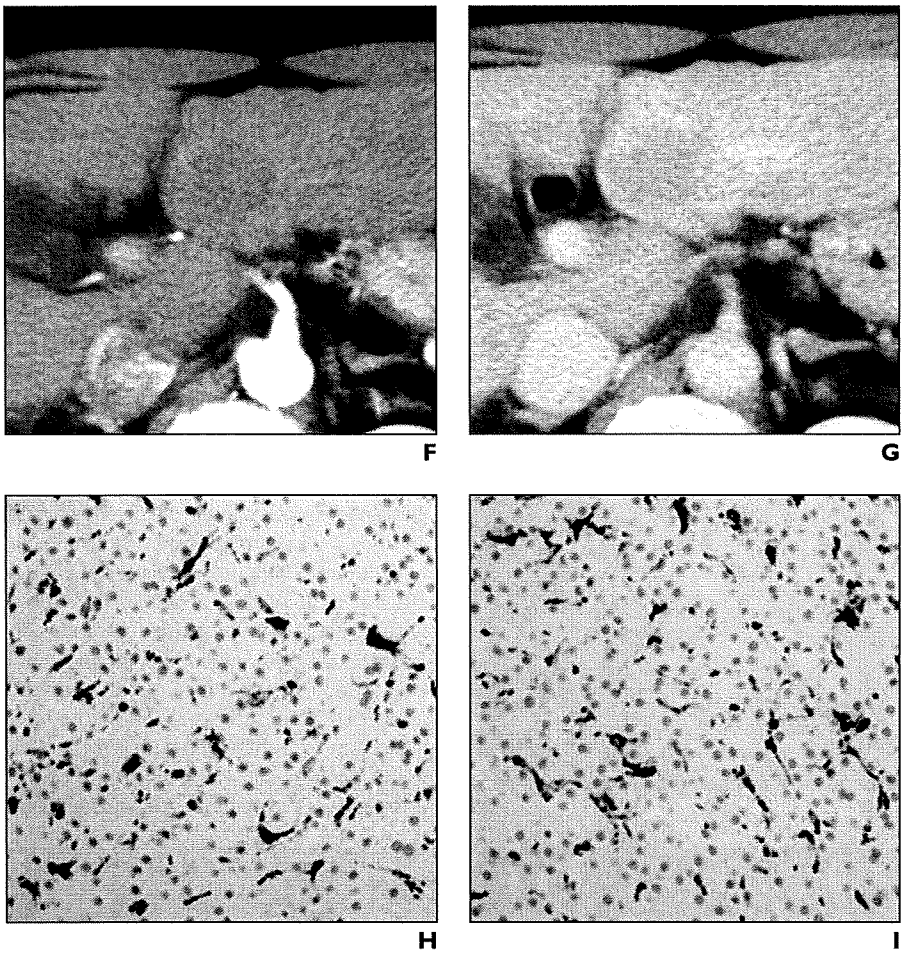

Fig. 2 (continued)—Case presentation of 61-year-old man with well-differentiated hepatocellular carcinoma.
F and **G**, On arterial phase (**F**) and portal phase (**G**) dynamic CT scans obtained 2 years after first examination (**A** and **B**), it is evident that intranodular hemodynamics and size of tumor have not changed compared with initial CT scans.
H and **I**, Photomicrographs of nontumorous (**H**) and tumorous (**I**) tissues from liver specimens show almost same number of CD68-positive Kupffer cells by immunohistochemical staining. Kupffer cell count ratio was 1.03.

of using liver parenchymal phase contrast-enhanced sonography to assess the histologic grades of nodular lesions associated with liver cirrhosis, such as dysplastic nodules and HCCs, and to determine whether this method could improve the accuracy of contrast-enhanced sonography in the differential diagnosis of nodular lesions in cirrhotic liver.

We used the advanced dynamic flow mode in this study. The advanced dynamic flow mode uses Doppler technique, but advanced dynamic flow images have higher resolution and less blooming area than conventional Doppler images. With the Doppler mode, poor resolution and large blooming areas present problems. In case of second-harmonic imaging and pulse-inversion imaging, tissue harmonic imaging (THI) becomes the problem because Levovist needs a high mechanical index. THI increases under the high-mechanical-index condition and interferes with the contrast image of Levovist. Also, bubbles of Levovist are easily collapsed under the high-mechanical-index condition, so it is hard to visualize the bubbles successively. The advanced dynamic flow mode has solved the problems mentioned, and the detectability of bubbles is superior to that of the other mode. Advanced dynamic flow is so sensitive that it can show the bubbles in real time.

Advanced dynamic flow has greatly improved the sensitivity of contrast-enhanced sonography in detecting the vascularity of hepatic nodules compared with conventional dynamic flow. In the contrast application, the advanced dynamic flow image looks very similar to a B-mode image thanks to the high resolution and wide dynamic range despite using Doppler technique. The detectability of the bubbles is better with advanced dynamic flow than with conventional dynamic flow. Therefore, advanced dynamic flow imaging can be used to detect bubbles in smaller vessels and has more penetration than conventional dynamic flow and shows uniform enhancement from shallow to deep regions. Thus, the advanced dynamic flow mode is very suitable for Levovist imaging.

Nicolau et al. [10] and Jang et al. [11] reported the usefulness of contrast-enhanced sonography in differentiating among histologic grades of hepatic tumors. The contrast agents that they used were SonoVue (Bracco), an aqueous suspension of phospholipid-stabilized microbubbles filled with sulfur hexafluoride, and Definity (Lantheus Medical Imaging), a perflutren lipid microsphere. These agents are blood pool contrast agents and cannot be taken up by the reticuloendothelial system (i.e., Kupffer cells) in liver parenchyma. From this point of view, these agents cannot be used to evaluate the reticuloendothelial function of a tumor. For the present study, we chose Levovist because it can be used to evaluate both vascular phase images (i.e., arterial phase and portal or late phase) and liver parenchymal phase images; Levovist is taken up to reticuloendothelial system after the dynamic phase. This difference in contrast agent is the most important and innovative point of our study compared with previous studies.

Estimation of the histologic grade of hepatic tumors by evaluating liver parenchymal phase images could lead to an improvement in the diagnosis of premalignant and borderline lesions and HCCs using contrast-enhanced sonography. In the present study, we found that the number of tumors showing isovascular staining in the liver parenchymal phase was decreased as nodules became less differentiated ($p < 0.05$, m × n chi-square test) and that Kupffer cell ratios in tumors that showed hypoperfusion in the liver parenchymal phase were significantly lower than in tumors that showed isoperfusion ($p < 0.05$, Mann-Whitney U test). These results suggest that liver parenchymal phase contrast-enhanced sonography is useful for assessing the histologic grade of HCCs and reflects reticuloendothelial function, and they support the hypothesis that liver parenchymal phase imaging is an independent method of diagnosis distinct from vascular phase imaging for the diagnosis of histologic grade

of premalignant and borderline lesions and HCCs. This peculiarity is similar to the phenomenon whereby stiff-shelled microbubbles SH U 563A (Sonovist, Schering) and NC100100 (Sonazoid, Daiichi-Sankyo, GE Healthcare) have been detected in Kupffer cells [12, 13]. Levovist enhances the liver and spleen but not the kidneys in the liver parenchymal phase. Alternatively, it is possible that sinusoids are found in the liver and spleen but not in malignant hepatic lesions and the kidneys.

Kono et al. [14] concluded in their study that the late parenchymal liver enhancement effect of AF0150 (Imavist, Alliance Pharmaceutical), another contrast agent, is not likely related to Kupffer cell uptake. Kupffer cells, the resident liver macrophages, constitute 31% of the sinusoidal cells [15]. They are more numerous (43%) in the periportal zone of the lobule. In addition to being more numerous, periportal Kupffer cells are larger, have more lysosomes, and take up more particles than do middle- or central-zone Kupffer cells [16]. Tanaka et al. [1] reported that cancerous tissue of well-differentiated HCCs possesses blood spaces that are similar to the normal sinusoids, but that as tumors grew in size and came to have a lower histologic grade, the blood spaces increased in apparent capillarization and became morphologically different from normal sinusoids. In addition, Sugihara et al. [17] reported that well-differentiated HCCs with indistinct margins grow by replacing surrounding liver cell cords on the boundary to noncancerous areas and that blood spaces in the tumor and surrounding sinusoids could be continuous. Therefore, blood spaces are expected to possess morphologic and functional characteristics similar to those of normal sinusoids. When neovascularization occurred, normal sinusoids were destroyed and the portal supply declined. Thereafter, reticuloendothelial cells lost their functional ability to take up microbubbles, resulting in the tumorous perfusion defects observed in liver parenchymal phase imaging. With this in mind, we speculate that nodules, such as dysplastic nodules and some well-differentiated HCCs, that possess portal areas and blood spaces similar to those of normal sinusoids may take up

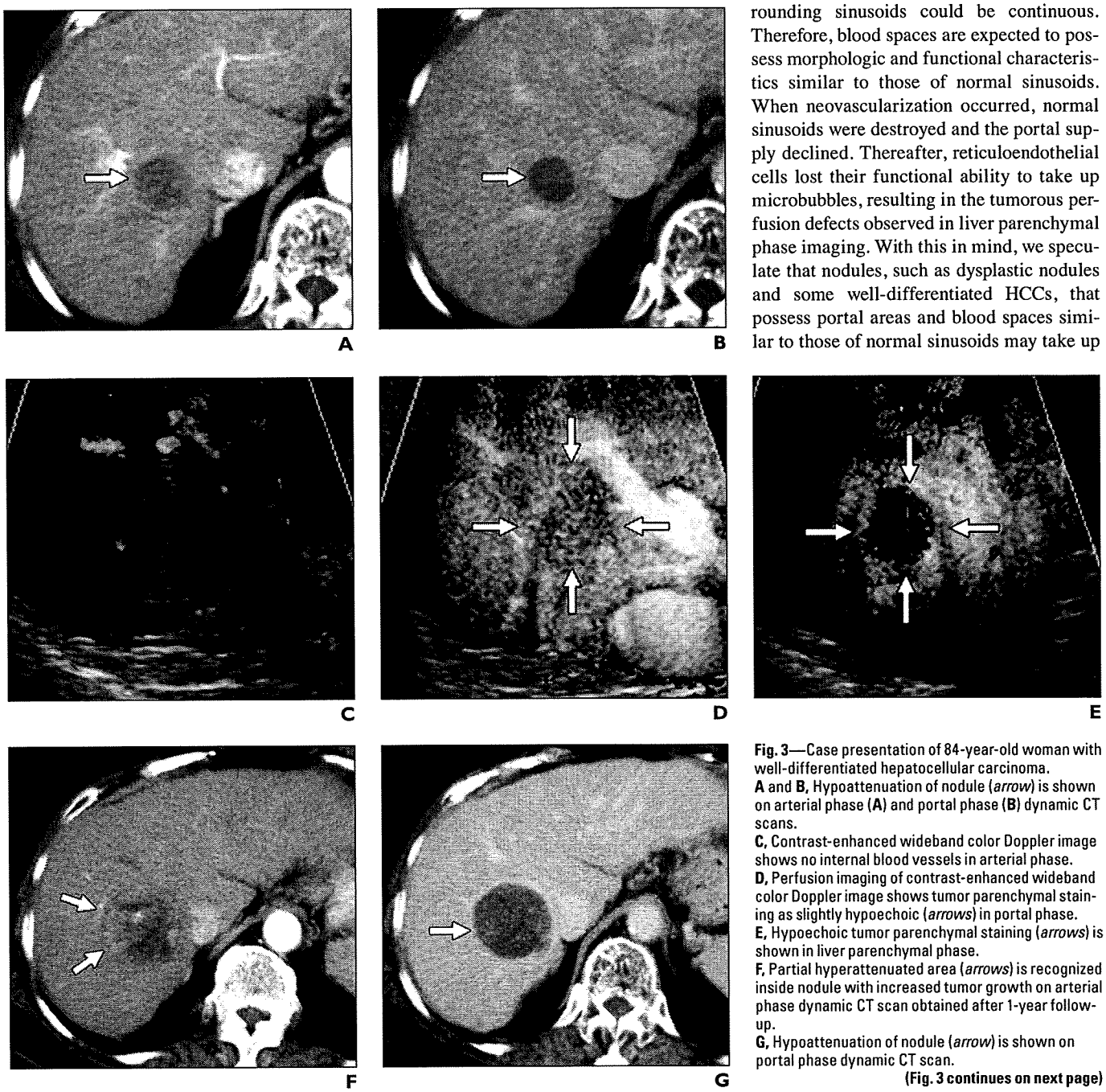

Fig. 3—Case presentation of 84-year-old woman with well-differentiated hepatocellular carcinoma.
A and **B**, Hypoattenuation of nodule (*arrow*) is shown on arterial phase (**A**) and portal phase (**B**) dynamic CT scans.
C, Contrast-enhanced wideband color Doppler image shows no internal blood vessels in arterial phase.
D, Perfusion imaging of contrast-enhanced wideband color Doppler image shows tumor parenchymal staining as slightly hypoechoic (*arrows*) in portal phase.
E, Hypoechoic tumor parenchymal staining (*arrows*) is shown in liver parenchymal phase.
F, Partial hyperattenuated area (*arrows*) is recognized inside nodule with increased tumor growth on arterial phase dynamic CT scan obtained after 1-year follow-up.
G, Hypoattenuation of nodule (*arrow*) is shown on portal phase dynamic CT scan.
(Fig. 3 continues on next page)

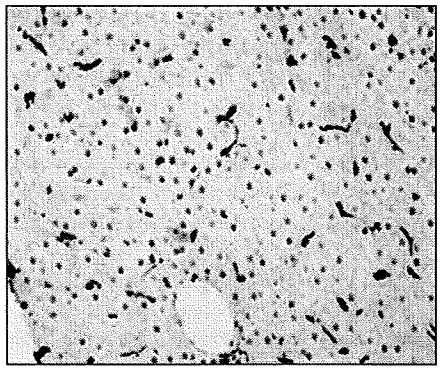

H

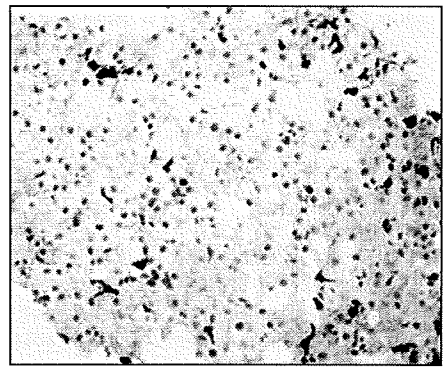

I

Fig. 3 (continued)—Case presentation of 84-year-old woman with well-differentiated hepatocellular carcinoma.
H and **I**, There were fewer CD68-positive Kupffer cells in nontumorous tissue (**H**) than in tumorous tissue (**I**) as shown by immunohistochemical staining of liver specimens. Kupffer cell count ratio was 0.59.

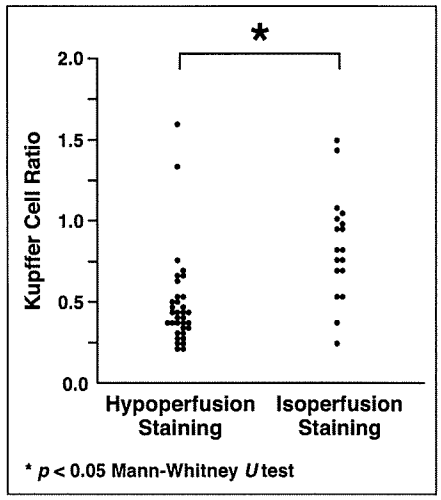

Fig. 4—Graph shows correlation between liver parenchymal phase imaging and Kupffer cell ratios. Kupffer cell ratios in tumors that showed hypoperfusion at liver parenchymal phase were significantly lower than those in tumors that showed isoperfusion ($p < 0.05$, Mann-Whitney *U* test).

microbubbles in a manner similar to nonnodular adjacent tissue. This idea is supported by the finding that all dysplastic nodules and 10 (53%) well-differentiated HCCs showed homogeneous isoperfusion relative to adjacent liver, but that no moderately and poorly differentiated HCCs showed homogeneous isoperfusion relative to adjacent liver. It was possible in this study to more precisely classify HCC tumors by using contrast-enhanced sonography to subdivide type 1 nodules into type 1a and type 1b and type 3 nodules into type 3a and type 3b, thereby improving diagnostic accuracy through the addition of liver parenchymal phase image evaluation.

In the present study, all dysplastic nodules and six HCCs (two type 3a and four type 3b well-differentiated HCCs) without treatment were monitored. This group is considered to be a low malignant grade with respect to intranodular hemodynamics because these nodules were hypovascular. This suggestion is supported by a previous report from Hayashi et al. [18] who analyzed the correlation between intranodular blood supply of borderline lesions (i.e., dysplastic nodules or well-differentiated HCCs) and their progression to hypervascular classic HCCs. They reported that the ratio of progression to classical HCC from a hypovascular tumor was 12.9% within 730 days and that hypovascular tumors required no expeditious treatment. It should be pointed out that this group could be further characterized by adding liver parenchymal phase contrast-enhanced sonography to allow type 3a nodules to be distinguished from type 3b. This distinction is important because during the 1-year follow-up period, both type 3a well-differentiated HCCs developed into overt HCCs that were perfused by only the hepatic artery, whereas all type 3b tumors (all dysplastic nodules and well-differentiated HCCs) exhibited no change in intranodular hemodynamics during the follow-up period. Therefore, it is altogether possible to accurately differentiate between the various tumorous biologic malignancy grades, make a more precise diagnosis, and adapt a patient's treatment accordingly.

The results of the present study also show that the use of liver parenchymal phase imaging with the already established diagnostic procedure, vascular phase contrast-enhanced sonography [3–6], may yield more detailed information about the multistep development of HCCs. In our study, 168 patients had a single hepatic nodule, 57 of whom underwent tumor biopsy or partial hepatectomy. One hundred eleven cases were diagnosed by a noninvasive imaging technique based on guidelines of the European Association for the Study of the Liver, American Association for the Study of Liver Diseases (AASLD), and Japan Society of Hepatology (JSH).

Kudo, Okanoue, and the JSH [19] reported the management of HCC in Japan. If a nodule shows the imaging findings typical of HCC (i.e., arterial phase hypervascularity with portal venous phase washout on dynamic CT or dynamic MRI) in a cirrhotic liver, the nodule is confirmed as HCC. AASLD guidelines [20] also indicate that if the radiologic appearance of the mass is suggestive of HCC (arterial hypervascularity with venous washout in cirrhotic liver), then the likelihood that the lesion is HCC is extremely high and biopsy is not essential. According to those guidelines, of the 111 patients with masses diagnosed as HCCs without pathologic results, 95 patients received radiofrequency ablation and 16 patients received partial hepatectomy (five well-differentiated HCCs, eight moderately differentiated HCCs, three poorly differentiated HCCs).

Several limitations exist in this study. The first limitation concerns the diagnosis of HCCs and dysplastic nodules because the diagnoses of 86% of the nodular lesions were made on the basis of needle biopsy specimens. To reduce sampling error to an acceptable minimum, at least two needle core biopsies were performed for each tumor; however, it is difficult to correctly diagnose the histologic grade of partially differentiating nodules, and therefore further study with additional resected specimens is needed. Second, only 14 tumors, six well-differentiated HCCs and eight dysplastic nodules, could be observed for a long follow-up period (i.e., ≥ 1 year). To clarify the usefulness of contrast-enhanced sonography in the diagnosis of premalignant and borderline lesions and overt HCCs, further case studies must be performed with a special focus on histopathologic correlation and a larger number of cases with a longer follow-up period.

Third, contrast-enhanced sonography cannot be applied to nodules that cannot be detected on B-mode sonography. In this respect, the method presented in this study may be inferior to CT or MRI but has great merit because it allows evaluation of intranodular hemodynamics and reticuloendothelial function in one series of contrast-enhanced sonography. By adding liver parenchymal phase imaging, we can assess the reticuloendothelial function of tumors. This technique seems to surpass current diagnostic methods that evaluate tumors using only vascular phase imaging. Hereafter, a second-generation contrast agent could be used that is taken up by the reticuloendothelial system of the liver and, in combination with contrast-enhanced sonography, might have the same degree of diagnostic utility as dynamic CT with superparamagnetic iron oxide–enhanced MRI together because both intranodular hemodynamics and reticuloendothelial function of tumors can be conveniently evaluated in one series of contrast-enhanced sonography.

In conclusion, liver parenchymal phase imaging may provide additional information that can be used to assess histologic grades of tumor, leading to an improvement in the differential diagnosis of nodular lesions associated with cirrhotic liver. Further case studies may be required in a larger number of cases for a longer follow-up period.

References

1. Tanaka M, Nakashima O, Wada Y, Kage M, Kojiro M. Pathomorphological study of Kupffer cells in hepatocellular carcinoma and hyperplastic nodular lesions in the liver. *Hepatology* 1996; 24:807–812
2. Kim AY, Choi BI, Kim TK, et al. Hepatocellular carcinoma: power Doppler US with a contrast agent—preliminary results. *Radiology* 1998; 209: 135–140
3. Kudo M. Imaging blood flow characteristics of hepatocellular carcinoma. *Oncology* 2002; 62: 48–56
4. Kudo M. *Contrast harmonic imaging in the diagnosis and treatment of hepatic tumors*. Tokyo, Japan: Springer-Verlag, 2003
5. Kudo M. Imaging diagnosis of hepatocellular carcinoma and premalignant/borderline lesions. *Semin Liver Dis* 1999; 19:297–309
6. Wen YL, Kudo M, Zheng RQ, et al. Characterization of hepatic tumors: value of contrast-enhanced coded phase-inversion harmonic angio. *AJR* 2004; 182:1019–1026 [Erratum in *AJR* 2004; 183:1175]
7. Pugh RNH, Murray-Lyon IM, Dawson JL, Pietroni MC, Williams R. Transection of the oesophagus for bleeding oesophageal varices. *Br J Surg* 1973; 60:646–669
8. [No authors listed]. Terminology of nodular hepatocellular lesions. International Working Party. *Hepatology* 1995; 22:983–993
9. Albrecht T, Hoffmann CW, Schettler S, Overberg A, Ilg M, Wolf KJ. Improved detection of liver metastases with phase inversion imaging during the liver-specific phase of the ultrasound contrast agent, Levovist. *Eur Radiol* 1999; 9[suppl 3]: S388
10. Nicolau C, Catalá V, Vilana R, et al. Evaluation of hepatocellular carcinoma using SonoVue, a second generation ultrasound contrast agent: correlation with cellular differentiation. *Eur Radiol* 2004; 14:1092–1099
11. Jang HJ, Kim TK, Burns PN, et al. Enhancement patterns of hepatocellular carcinoma at contrast-enhanced US: comparison with histologic differentiation. *Radiology* 2007; 244:898–906
12. Bauer A, Blomley M, Leen E, Cosgrove D, Schlief R. Liver-specific imaging with SHU 563A: diagnostic potential of a new class of ultrasound contrast media. *Eur Radiol* 1999; 9[suppl 3]:S349–S352
13. Marelli C. Preliminary experience with NC100100, a new ultrasound contrast agent for intravenous injection. *Eur Radiol* 1999; 9[suppl 3]:S343–S346
14. Kono Y, Gregory CS, Thomas P, et al. Mechanism of parenchymal enhancement of the liver with a microbubble-based US contrast medium: an intravital microscopy study in rats. *Radiology* 2002; 224:253–257
15. Bouwens L, Baekeland M, De Zanger R, Wisse E. Quantitation, tissue distribution and proliferation kinetics of Kupffer cells in normal rat liver. *Hepatology* 1986; 6:718–722
16. Ruttinger D, Vollmar B, Wanner GA, et al. In vivo assessment of hepatic alterations following chloride-induced Kupffer cell blockade. *J Hepatol* 1996; 25:960–967
17. Sugihara S, Kojiro M, Nakashima T. Ultrastructural study of hepatocellular carcinoma with replacing growth pattern. *Acta Pathol Jpn* 1985; 35:549–559
18. Hayashi M, Matsui O, Ueda K, Kawamori Y, Gabata T, Kadoya M. Progression to hypervascular hepatocellular carcinoma: correlation with intranodular blood supply evaluated with CT during intraarterial injection of contrast material. *Radiology* 2002; 225:143–149
19. Kudo M, Okanoue T; Japan Society of Hepatology. Management of hepatocellular carcinoma in Japan: consensus-based clinical practice manual proposed by the Japan Society of Hepatology. *Oncology* 2007; 72[suppl 1]:2–15
20. Bruix J, Sherman M. Management of hepatocellular carcinoma. *Hepatology* 2005; 42:1208–1236

SPECIAL ARTICLE

Pathologic Diagnosis of Early Hepatocellular Carcinoma: A Report of the International Consensus Group for Hepatocellular Neoplasia

International Consensus Group for Hepatocellular Neoplasia

See Editorial on Page 355

Advances in imaging techniques and establishment of surveillance protocols for high-risk populations have led to the detection of small hepatic nodules in patients with chronic liver diseases, particularly those with cirrhosis or chronic hepatitis caused by hepatitis B or C viruses. These nodules, comprising a broad range of diagnostic entities—some benign and some with malignant potential—are currently defined histologically, and their clinical management often depends on the ability to make a reliable histologic diagnosis.

Evidence accumulated in the last two decades strongly favors the existence of a sequence of events in hepatic nodules that precedes the emergence of hepatocellular carcinoma (HCC),[1-10] and these lesions are recognized as precursors of HCC. However, from the beginning of their recognition, there has been considerable confusion concerning nomenclature and diagnostic approaches to these hepatic nodules. To clarify these issues, an International Working Party (IWP) of the World Congresses of Gastroenterology proposed a consensus nomenclature and diagnostic criteria for hepatocellular nodular lesions in 1995.[11] The IWP classified nodular lesions found in chronic liver disease into large regenerative nodule, low-grade dysplastic nodule (L-DN), high-grade dysplastic nodule (H-DN), and HCC; this nomenclature has been widely adopted. In addition, the IWP introduced the concept of dysplastic focus as a cluster of hepatocytes with features of early neoplasia (in particular small cell change or iron-free foci in a siderotic background) measuring less than 0.1 cm, and defined small HCC as a tumor measuring less than 2 cm.

More recent studies support the division of small HCC into two clinico-pathological groups that have been termed early HCC and progressed HCC. Early HCC has a vaguely nodular appearance and is well differentiated. Progressed HCC has a distinctly nodular pattern and is mostly moderately differentiated, often with evidence of microvascular invasion.[12] Early HCC has a longer time to recurrence and a higher 5-year survival rate compared with progressed HCC.[13]

Small lesions with malignant potential have only subtle differences from the surrounding parenchyma, making them difficult to assess reproducibly. Differences in the application of diagnostic criteria between Western and Eastern pathologists has been a persistent difficulty in research and clinical management of these lesions.[14] In order to obtain a refined and up-to-date international consensus on the histopathologic diagnosis of nodular lesions, such as dysplastic nodules and early HCC, the International Consensus Group for Hepatocellular Neoplasia (ICGHN) was convened in April 2002 in Kurume, Japan. The group has met several times up to July 2007 under the auspices of the Laennec Liver Pathology Society. The ICGHN is currently comprised of 34 pathologists and two clinicians from 13 countries. It includes most members of the original IWP who are still active and all the participants from the first ICGHN meeting. This consensus document summarizes the results of our meetings.

Materials and Methods

Twenty-six resected cases of nodules from 23 patients with chronic hepatitis or cirrhosis caused by hepatitis B or

Abbreviations: GPC3, glypican-3; GS, Glutamine synthetase; HCC, hepatocellular carcinoma; H-DN, high-grade dysplastic nodule; HSP70, heat shock protein 70; ICGHN, The International Consensus Group for Hepatocellular Neoplasia; IWP, International Working Party; L-DN, low-grade dysplastic nodule.

From the Department of Pathology, Kurume University, Kurume, Japan.

Received June 11, 2008; accepted October 16, 2008.

The International Consensus Group for Hepatocellular Neoplasia consists of: Masamichi Kojiro, Ian R. Wanless, Venancio Alves, Sunil Badve, Charles Balabaud, Pierre Bedosa, Prithi Bhathal, Paulette Bioulac-Sage, Elizabeth M. Brunt, Alastair D. Burt, John R. Craig, Amar Dhillon, Linda Ferrell, Stephen A. Geller, Zackary D. Goodman, Annette S. H. Gouw, Maria Guido, Maha Guindi, Prodromos Hytiroglou, Masayoshi Kage, Fukuo Kondo, Masutoshi Kudo, Gregory Y. Lauwers, Masayuki Nakano, Valerie Paradis, Young-Nyun Park, Alberto Quaglia, Massimo Roncalli, Tania Roskams, Boris Ruebner, Michiie Sakamoto, Romil Saxena, Neil D. Theise, Swan Thung, and Dina Taniakos.

Address reprint requests to: Masamichi Kojiro, M.D., Department of Pathology, Kurume University, 67 Asahi-machi, Kurume-shi 830-0011, Japan. E-mail: kojiro@med.kurume-u.ac.jp; fax: (81)-942-31-7726.

Published online in Wiley InterScience (www.interscience.wiley.com).

DOI 10.1002/hep.22709

Potential conflict of interest: Nothing to report.

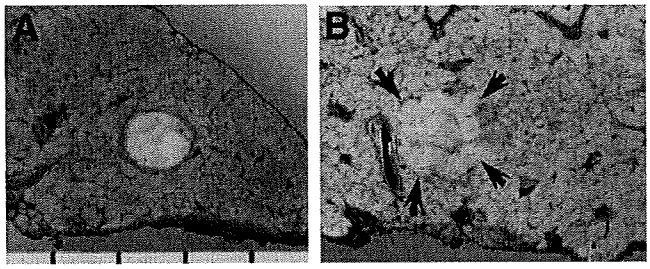

Fig. 1. (A) HCC of distinctly nodular type (progressed HCC), 12 mm in diameter. There was no discrepancy in the diagnosis of HCC with this growth pattern despite the small tumor size. (B) Small HCC of vaguely nodular type (early HCC) (arrows). These lesions were often a diagnostic problem, solved in part by recognition of the histologic features of stromal invasion.

C virus were selected from one Korean and two Japanese medical centers. All the lesions measured less than 2 cm in diameter. One hematoxylin and eosin–stained slide comprising the entire width of each lesion, a gross picture, and brief clinical data were reviewed by each pathologist individually, and the lesions were classified according to the IWP criteria. The group met at Kurume University Medical School, Kurume, Japan, in April 2002 to review all the lesions with photographs and by group review of relevant slides with a projecting microscope. The histologic diagnostic criteria were discussed, focusing on cases with marked discrepancies in initial, premeeting diagnosis. The second meeting was held at the University of Leuven, Belgium, in May 2004. The members discussed the diagnosis of an additional set of 22 resected small nodules. The third meeting was held at the Aristotle University of Thessaloniki, Greece in May 2006, and histopathologic consensus on both dysplastic nodules and early HCC was obtained. Kappa statistics were obtained from the comparative diagnostic panels of the first two of these meetings using SAS software version 8.2 (SAS Institute Inc., Cary, NC).

Summary of Comparative Diagnosis Data from Two Rounds of Slide Circulation

There was little difficulty in agreeing on the diagnosis of well-differentiated, small HCC of the distinctly nodular type or when the tumor was moderately differentiated HCC (Fig. 1A). The overwhelming diagnostic challenge was the differentiation of H-DNs from well-differentiated, small HCC of the vaguely nodular type (early HCC) (Fig. 1B). These lesions showed the lowest kappa value at the first conference with wide interobserver variation on initial review; the variation was diminished, but not totally resolved after the first conference. Initially, Asia-trained pathologists generally diagnosed HCC more frequently than Western pathologists. After the first conference, this discrepancy decreased, and kappa values for HCC rose from 0.30 to 0.49 (though with different slide sets), with most Western pathologists ultimately agreeing with the diagnosis of HCC. The improvement of diagnostic agreement after the initial conference was due to the recognition of stromal invasion as a criterion for diagnosis of well-differentiated HCC. Stromal invasion is defined as tumor cell invasion into the portal tracts or fibrous septa within vaguely nodular lesions[15,16] (Fig. 2).

Current Suggestions for Diagnostic Criteria

Gross and Radiographic Features

It is often possible to make a presumptive diagnosis of HCC when a small lesion is distinctly nodular and is hypervascular on contrast-enhanced imaging in the setting of cirrhosis.[17,18] However, errors will occur occasionally with this approach. It has been reported that a small but significant proportion of explant livers was misdiagnosed as HCC.[19] Any focal lesion containing a large arterio-venous shunt may be hypervascular (for example, focal nodular hyperplasia[20] or similar lesions[21]). A hypovascular lesion less than 2 cm having a vaguely nodular appearance cannot be accurately diagnosed by gross examination or imaging. Such lesions should undergo guided needle core biopsy.

Some small nodules have a "nodule-in-nodule" appearance either radiologically or on gross examination.[22] In this situation, the subnodule usually represents dedifferentiation of the "parent" nodule. The parent nodule may be a dysplastic nodule or well-differentiated HCC, and the subnodule is invariably a less-differentiated lesion. In these situations, the entire nodule is classified by the worst component. Typically, the less-differentiated component is more vascular than the parent component.[23-27] However, if the parent nodule is a dysplastic nodule and the subnodule is well-differentiated HCC, the subnodule may not be hypervascular, because unpaired arteries have not yet developed. Such unpaired arteries are small arteries (unaccompanied by bile duct) occurring

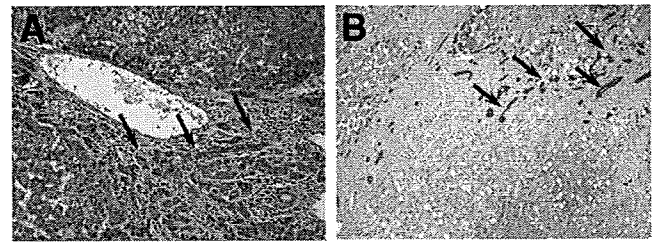

Fig. 2. (A) Stromal invasion in early HCC. The tumor cells (arrows) are invading an intratumoral portal tract. (B) CK19 immunostaining of another lesion. The ductular reaction (arrows) is mimicking stromal invasion and is prominent at the stroma-parenchymal interface. Well-differentiated HCC with fatty change is located at the bottom half of the image.

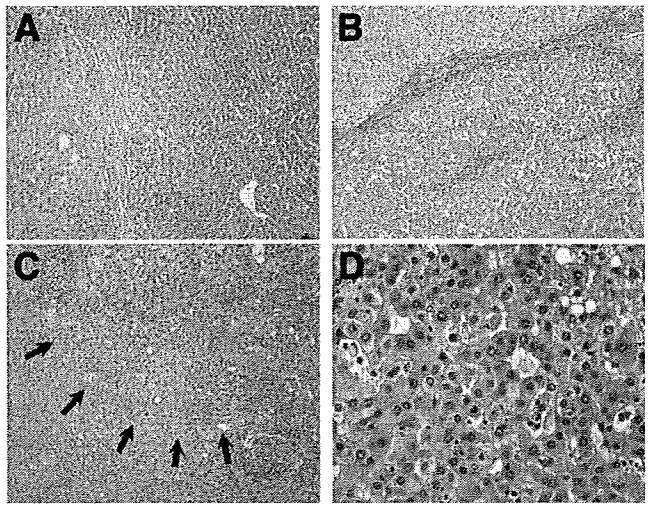

Fig. 3. (A) Low-grade dysplastic nodule (right two-thirds) shows mild increase in cell density with a clearer trabecular arrangement than the adjacent parenchyma. (B) High-grade dysplastic nodule. The cell density in this example is more than 1.5 times higher than that in the surrounding tissue (upper left). Irregularity of the trabecular pattern is remarkable, but there is no obvious infiltrative growth. (C, D) Small, well-differentiated HCC of vaguely nodular type (early HCC). The tumor shows replacing growth at the boundary (arrows), and the cell density is more than 2 times higher than that in the surrounding tissue. The tumor cells show an irregular thin-trabecular pattern with occasional pseudoglands. Stromal invasion was present elsewhere in the tumor.

outside the original portal tracts, and are indicative of neovascularization. They have a thin muscular wall that can be recognized in more detail via immunostaining for α-smooth muscle actin. Regardless of vascularity, a nodule-in-nodule appearance suggests the presence of HCC.

Pathologic Features

Low-Grade Dysplastic Nodules. L-DNs are sometimes vaguely nodular but are often distinct from the surrounding cirrhotic liver because of the presence of peripheral fibrous scar. This is not a true capsule, but rather condensation of scarring as is seen around all cirrhotic nodules. L-DNs show mild increase in cell density with a monotonous pattern, and they have no cytologic atypia, though they may have large cell change (formerly referred to as large cell dysplasia[28]). Architectural changes beyond clearly regenerative features are not present; these lesions do not contain pseudoglands or markedly thickened trabeculae (Fig. 3). Unpaired arteries are sometimes present in small numbers.[29] Nodule-in-nodule lesions are not present in L-DNs. L-DNs may have diffuse siderosis or diffusely increased copper retention.

Among members of the consensus panels, there was no serious difficulty in differentiating L-DNs from early HCC. At the opposite end of the spectrum, distinction between L-DNs and large regenerative nodules was often found to be difficult or impossible. Therefore, there is currently consensus that distinction between these two diagnostic categories cannot be made confidently by morphology alone and remains a task for the future. Fortunately, this distinction does not appear to have significant practical consequences at present.

High-Grade Dysplastic Nodules. H-DNs may be distinctly or vaguely nodular in the background of cirrhosis, although they also lack a true capsule, similar to L-DNs; however, they are more likely to show a vaguely nodular pattern than L-DNs. An H-DN is defined as having architectural and/or cytologic atypia, but the atypia is insufficient for a diagnosis of HCC. These lesions most often show increased cell density, sometimes more than 2 times higher than the surrounding nontumoral liver, often with an irregular trabecular pattern (Fig. 3). Small cell change (also known as small cell dysplasia[30]) is the most frequently seen form of cytologic atypia in H-DNs. This form of atypia may also occur in small hepatocellular foci outside of H-DNs; the term dysplastic focus[11] may be appropriately used for such lesions. Large cell change may or may not be present in H-DNs. Unpaired arteries are found in most lesions, but usually not in great numbers. A nodule-in-nodule appearance is occasionally found in H-DNs, and subnodules often have a higher labeling index of Ki-67 or proliferating cell nuclear antigen than that of H-DN parenchyma. When a nodule with largely H-DN features contains a subnodule of HCC, the subnodule of HCC is usually well-differentiated with a well-defined margin.

The diagnostic discrepancy between H-DN and early HCC was frequent at the first consensus meeting, but was remarkably improved at the second meeting due to the recognition of stromal invasion as a diagnostic criterion for the differentiation of H-DN from early HCC. If areas of questionable invasion are present, immunostaining for keratins 7 or 19 may be useful; if such staining demonstrates a ductular reaction, the focus is considered a pseudoinvasion and does not warrant a diagnosis of HCC[31] (Fig. 2B).

Early HCC (Small Well-Differentiated HCC of Vaguely Nodular Type)

Early HCC tumors are vaguely nodular and are characterized by various combinations of the following major histologic features[6,22,32] (Fig. 3):

(1) increased cell density more than 2 times that of the surrounding tissue, with an increased nuclear/cytoplasm ratio and irregular thin-trabecular pattern;

(2) varying numbers of portal tracts within the nodule (intratumoral portal tracts);

(3) pseudoglandular pattern;

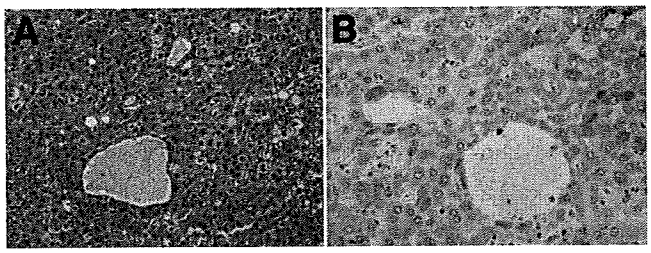

Fig. 4. GPC3 expression in small, well-differentiated HCC of vaguely nodular type (early HCC). (A) Hematoxylin-eosin stain. (B) Immunostaining for GPC3 shows expression in the cytoplasm of tumor cells.

(4) diffuse fatty change; and
(5) varying numbers of unpaired arteries.

Among these features, diffuse fatty change is observed in approximately 40% of cases.[33] The characteristic features of early HCC are sometimes seen in larger tumors as well—that is, well-differentiated tumors that measure over 2 cm and thus do not qualify for the designation of small HCC set forth by the IWP. The prevalence of fatty change decreases along with increasing tumor size; therefore, fatty change is uncommon in tumors larger than 3 cm. Fatty change is also uncommon in moderately differentiated HCCs. Any of the features listed above may be diffuse throughout the lesion or may be restricted to an expansile subnodule (nodule-in-nodule). Most importantly, because all of these features may also be found in H-DNs, it is important to note that stromal invasion remains most helpful in differentiating early HCC from H-DNs.

Emerging Tumor Markers

Alpha-fetoprotein is a well-established serum marker for HCC. However, elevated levels are rarely found in early HCCs. Alpha-fetoprotein is not useful as a tissue marker because of low sensitivity (25% to 30%), even with moderately differentiated HCC.

Glypican-3 (GPC3), a cell-surface heparan sulfate proteoglycans that is secreted into the plasma, has recently become established as a serum and tissue marker for HCC.[34-39] GPC3 immunoreactivity has a reported sensitivity of 77% and specificity of 96% in the diagnosis of small HCC; therefore, GPC3 positivity is a strong argument for malignancy.[40,41] The staining pattern is usually cytoplasmic but may be membranous or canalicular (Fig. 4). The monoclonal antibody from Biomosaics (IG12 clone) at a dilution of 1/50 to 1/100 as amplified with the new short polymer systems (Advance [Dako], Novolink [Novocastra], and Super-picture + [Zymed]) yields reliable results. Because GPC3 staining may be only focal, additional markers or a panel of markers may be necessary. GPC3 staining must be interpreted in context, because it may also be seen in regenerating hepatocytes in a setting of hepatitis[42] and in melanocytic lesions.[43]

Heat shock protein 70 (HSP70) belongs to a class of genes (heat shock proteins) implicated in the regulation of cell cycle progression, in apoptosis, and in tumorigenesis.[44-46] Most HCCs are associated with chronic inflammation and fibrosis acting as stressful conditions that lead to heat shock protein synthesis. HSP70 is, in particular, a potent antiapoptotic survival factor. Chuma et al.[47] reported HSP70 as the most abundantly up-regulated gene among a set of 12,600 genes in early HCC. Furthermore, it was significantly overexpressed in progressed HCC as compared with early HCC, and in the latter as compared with precancerous lesions. HSP70 immunoreactivity was recently reported in the majority of HCCs, including early and well-differentiated forms, but not in nonmalignant nodules,[48] thus suggesting its use as a marker of malignancy. HSP70 immunoreactivity (SC-24, dilution 1:250 to 1:500 amplified with short polymer systems; Santa Cruz Biotechnology, Santa Cruz, CA) is nucleocytoplasmic and mostly focal with 70% sensitivity for HCC detection in surgically resected specimens.[49]

Glutamine synthetase (GS) catalyzes the synthesis of glutamine from glutamate and ammonia in the mammalian liver[49] where it has been shown to be restricted to hepatocytes surrounding the terminal hepatic venules.[50] It is known that glutamine, the end product of GS activity, is the major energy source of tumor cells.[51] Most importantly, GS is a target gene of β-catenin so that its overexpression is associated with mutations of β-catenin or with activation of this pathway.[52-54] Up-regulation of GS messenger RNA, protein, and activity were shown by Christa et al.[52] in human HCC, while Osada et al.[55] reported the stepwise increase in GS immunoreactivity from precancerous lesions to early HCC to progressed HCC. The monoclonal antibody from Chemicon International (clone MB302) at a dilution of 1/500 to 1/1000 and amplified with a new short polymer system yields reliable results. In order to increase its specificity as a marker of malignancy, GS immunostaining should be diffuse and of strong intensity, a pattern that can be seen in 50% of HCCs, including early forms.[49]

The combination of more than one putative marker of malignancy raises the overall accuracy. When applying a panel of these three markers (GPC3, HSP70, and GS) to resected small lesions, the finding of any two positive markers had a sensitivity of 72% and a specificity of 100% to detect malignancy.[48] The diagnostic accuracy of this panel of markers in liver biopsies of hepatocellular nodules has not been yet tested.

Comment

The IWP criteria of 1995 have led to remarkable progress in global standardization of nomenclature of liver nodules.[11] However, although these criteria have been widely adopted, their application is challenging in equivocal lesions. Perhaps the most significant problem is that most histologic criteria are arrayed on a gradual spectrum and cannot be easily summarized as present or absent. Additionally, the number of criteria suggested in the literature are too numerous to achieve interobserver consensus, and the diagnostic weight carried by each of these criteria is uncertain. Frequently used criteria for malignancy in other tissues, such as mitotic activity and cellular atypia, are not represented to a significant degree in well-differentiated HCC. In addition, because the liver lacks a layered structure as seen in the gastrointestinal tract, it is difficult to determine the presence of destructive growth in early HCCs.

Despite these difficulties, current histologic criteria for these nodules clearly yield reliable diagnoses at both ends of the spectrum; most pathologists will correctly identify nodules up to L-DN as benign, whereas even small well-differentiated nodules with distinct nodular pattern or small moderately differentiated HCCs will be correctly identified as malignant. The remaining gray zone includes H-DN and early HCC. In evaluation of these lesions, the presence of stromal invasion is a useful criterion of malignancy.[15,16] Accordingly, pathologists can decide whether the equivocal tumor is HCC or H-DN by recognizing the presence or absence of tumor cell invasion into the intratumoral portal tracts. When obvious stromal invasion is not found in an equivocal tumor, the lesion may be diagnosed as either H-DN or early HCC without detectable invasion. The diagnosis of stromal invasion is subjective and may require the assistance of histochemical (Victoria Blue or reticulin stains[16]) and immunohistochemical stains (keratin 7 or 19) for differentiation from pseudoinvasion.[29] New immunohistochemical and molecular markers are still under investigation and are likely to prove useful.[46,54,56]

Role of Liver Biopsy. Regarding the application of biopsy for small nodules, the American Association for the Study of Liver Diseases recommends that biopsy should be performed for nodules less than 2 cm if their radiologic findings are not characteristic of HCC, whereas biopsy is not needed for lesions showing characteristic radiologic findings.[17] This recommendation has been supported by prospective validation.[18] Biopsy diagnosis of equivocal nodules remains a challenge, because minute biopsy specimens may not contain intratumoral portal tracts, thus precluding the detection of stromal invasion.

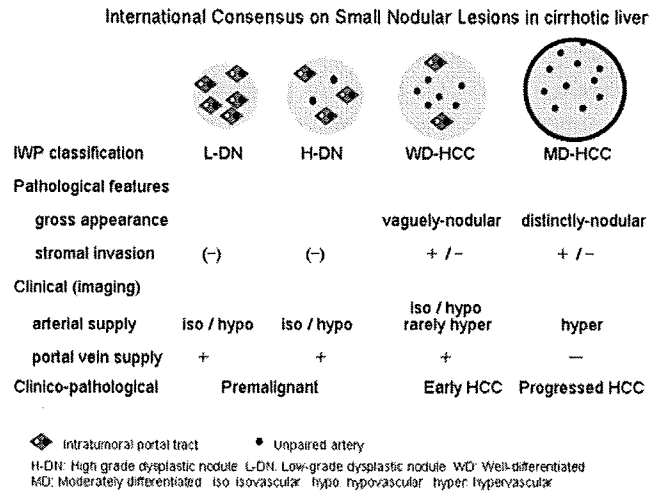

Fig. 5. Diagram summarizing clinical and pathological correlations. The cartoons in the top row show the anatomic changes that are found with the evolution of fully malignant HCC. Because early HCCs grow in a replacing pattern at the boundary, with tumor cells replacing the surrounding liver cell cords, they show a vaguely nodular appearance. When the tumors reach 1.5 to 2 cm in diameter, they tend to de-differentiate, becoming moderately differentiated and growing in an expansile fashion with formation of a fibrous capsule. Hypovascularity, hypervascularity, and isovascularity are understood to mean the signal intensity in the arterial phase of contrast-enhanced imaging relative to the nontumorous liver. Hypervascularity is related to the development of unpaired arteries, the absence of portal vein supply, and the distinctly nodular growth. The diagnosis must consider the context of the lesion, especially the presence of cirrhosis, the imaging findings, and the growth rate. In the appropriate context, a lesion with decreased portal vein supply without hypervascularity is suggestive of early HCC.

Similarly, the detection of unpaired arteries, mitoses, and various immunohistochemical markers are prone to sampling error. Core liver biopsy is definitely superior to fine needle aspiration, because the specimen obtained is suitable for the assessment of both architectural and cytologic features. Furthermore, the tissue block obtained provides materials for marker studies. Fine needle aspiration is usually adequate for the evaluation of large lesions that are likely to be moderately to poorly differentiated, where diagnostic criteria are easier to evaluate.

Clinico-pathological Correlation. Clinical and pathological features of early hepatocellular neoplasia are summarized in Fig. 5. The characteristic imaging appearance of HCC is a hypervascular lesion that shows washout in the portal venous phase. This appearance is also typical in small HCC of the distinctly nodular type and most moderately differentiated small HCCs. Dysplastic nodules and most early HCCs are hypovascular lesions. These classic images are explained by the anatomic features of the lesions. Taken together, the pathologic and imaging features define three phases in the evolution of neoplasia in cirrhotic liver, where dysplastic nodules represent the premalignant phase, well-differentiated HCC of the

vaguely nodular type represents early carcinoma, and small HCCs of the distinctly nodular type and moderately differentiated HCCs represent progressed carcinoma. In the noncirrhotic liver, however, the developmental process of HCC in humans has not been clarified.

Acknowledgment: The authors thank Mr. Kazuhiro Abe for kappa statistics.

References

1. Arakawa M, Kage M, Sugihara S, Nakashima T, Suenaga M, Okuda K. Emergence of malignant lesions within an adenomatous hyperplastic nodules in a cirrhotic liver. Observation in five cases. Gastroenterology 1986; 91:198-208.
2. Sakamoto M, Hirohashi S, Shimamoto Y. Early stages of multistep hepatocarcinogenesis: adenomatous hyperplasia and early hepatocellular carcinoma. Hum Pathol 1991;22:172-178.
3. Borzio M, Bruno S, Roncalli M, Mels GC, Ramella G, Borzio F, et al. Liver cell dysplasia is a major risk factor for hepatocellular carcinoma in cirrhosis: a prospective study. Gastroenterology 1995;108:812-817.
4. Le Bail B, Bernard PH, Balabaud C, Bioulac-Sage P. Prevalence of liver cell dysplasia and association with HCC in a series of 100 cirrhotic liver explants. J Hepatol 1997;27:835-842.
5. Libbrecht L, Craninx M, Nevens F, Desmet V, Roskams T. Predictive value of liver cell dysplasia for development "of hepatocellular carcinoma in patients with non-cirrhotic and cirrhotic chronic viral hepatitis. Histopathology 2001;39:66-73.
6. Hytiroglou P. Morphological changes of early human hepatocarcinogenesis. Semin Liver Dis 2004;24:65-75.
7. Libbrecht L, Desmet V, Roskams T. Preneoplastic lesions in human hepatocarcinogenesis. Liver Int 2005;25:16-27.
8. Theise ND, Park YN, Kojiro M. Dysplastic nodules and hepatocarcinogenesis. Clin Liver Dis 2002;6:497-512.
9. Paradis V, Laurendeau I, Vidaud M, Bedossa P. Clonal analysis of macronodules in cirrhosis. HEPATOLOGY 1998;28:953-958.
10. Plentz RR, Park YN, Lechel A, Kim H, Nellessen F, Langkopf BH, et al. Telomere shortening and p21-checkpoint inactivation characterize multistep hepatocarcinogenesis in humans. HEPATOLOGY 2007;45:968-976.
11. International Working Party. Terminology of nodular hepatocellular lesions. HEPATOLOGY 1995;22:983-993.
12. Kojiro M, Nakashima O. Histopathologic evaluation of hepatocellular carcinoma with a special reference to small early stage tumor. Semin Liver Dis 1999;19:287-296.
13. Takayama T, Makuuchi M, Hirohashi S, Sakamoto M. Early hepatocellular carcinoma as an entity with high rate of surgical cure. HEPATOLOGY 1998;28:1241-1246.
14. Kojiro M. Diagnostic discrepancy of early hepatocellular carcinoma between Japan and West. Hepatology Res 2007;37:S249-S252.
15. Kondo F, Kondo Y. Nagato Y, Tomizawa M, Wada K. Interstitial tumor cell invasion in small hepatocellular carcinoma. Evaluation in microscopic and low magnification view. J Gastroenterol Hepatol 1994;9:604-612.
16. Nakano M, Saito A, Yamamoto M, Doi M, Takasaki K. Stromal invasion and blood vessel wall invasion in well differentiated hepatocellular carcinoma. Liver 1997;17:41-46.
17. Bruix J, Sherman M. Management of hepatocellular carcinoma. HEPATOLOGY 2005;42:1208-1236.
18. Forner A, Vilana R, Ayuso C, Bianchi L, Sole M, Ramon J, et al. Diagnosis of hepatic nodules 20 mm or smaller in cirrhosis: prospective validation of the noninvasive diagnostic criteria for hepatocellular carcinoma. HEPATOLOGY 2008;47:97-104.
19. Hayashi PH, Trotter J, Forman L, Kugelmas M, Strinberg T, Russ P, et al. Impact of pretransplant diagnosis of hepatocellular carcinoma on cadveric liver allocation in the era of MELD. Liver Transpl 2004;10:42-48.
20. Wanless IR, Sapp H, Guindi M, Olshansky D, Takayama A. The pathogenesis of focal nodular hyperplasia: an hypothesis based on histologic review of 20 lesions including 3 occurring in early biliary cirrhosis. HEPATOLOGY 2006;44:491A.
21. Libbrecht L, Cassiman D, Verslype C, Maleux G, Van Hees D, Porenne J, et al. Clinicopathological features of focal nodular hyperplasia-like nodules. Am J Gastroenterol 2006;101:2341-2346.
22. Kojiro M. Pathology of Hepatocellular Carcinoma. Oxford: Blackwell Publishing, 2006.
23. Matsui O, Takashima T, Kadoya M, Ida M, Suzuki M, Kitagawa K, et al. Dynamic computed tomography during arterial portography: the most sensitive examination for small hepatocellular carcinoma. J Comput Assist Tomogr 1985;9:19-24.
24. Kudo M, Tomita S, Tochio H, Mimura J, Okabe Y, Kashida H, et al. Small hepatocellular carcinoma: diagnosis with US angiography with intra-arterial CO2 gas microbubles. Radiology 1992;182:155-160.
25. Bennett GL, Krinsky GA, Abitbol RJ, Kim SY, Theise ND, Teperman LW, et al. Ultrasound detection of hepatocellular carcinoma and dysplastic nodules in patients with cirrhosis: correlation of pretransplant ultrasound findingss and liver explant pathology in 200 patients. AJR Am J Roentgenol 2002;179:75-80.
26. Krinsky GA, Lee VS, Theise ND, Weinreb J, Morgan GR, Diflo T, et al. Hepatocellular carcinoma and dysplastic nodules in patients with cirrhosis: prospective diagnosis with MR imaging and explant correlation. Radiology 2001;219:445-454.
27. Van den Bos IC, Hussain SM, Terkivatan T, Zondervan PE, de Man RA. Stepwise carcinogenesis of hepatocellular carcinoma in the cirrhotic liver: demonstration on serial MR imaging. J Magn Reson Imaging 2006;24: 1071-1080.
28. Anthony PP, Vogel CL, Barker LE. Liver cell dysplasia: a premalignant condition. J Clin Pathol 1973;26:217-223.
29. Park YN, Yang C-P, Fernandez GJ, Cubukcu O, Thung SN, Theise ND. Neoangiogenesis and sinusoidal "capillarization" in dysplastic nodules of the liver. Am J Surg Path 1998;22:656-662.
30. Watanabe S, Watanabe S, Okita K, Harada T, Kodama T, Numa Y, et al. Morphologic studies of the liver cell dysplasia. Cancer 1983;51:2197-2205.
31. Park YN, Kojiro M, Di Tommaso L, Dhillon AP, Kondo F, Nakano M, et al. Ductular reaction is helpful in defining early stromal invasion, small hepatocellular carcinomas, and dysplastic nodules. Cancer 2007;109:915-923.
32. Hytiroglou P, Park YN, Krinsky G, Theise ND. Hepatic precancerous lesions and small hepatocellular carcinoma. Gasteroenterol Clin N Am 2007;36:867-887.
33. Kutami R, Nakashima Y, Nakashima O, Shiota K, Kojiro M. Pathomorphologic study on the mechanism of fatty change in small hepatocellular carcinoma of humans. J Hepatol 2000;33:282-289.
34. Capurro M, Wanless IR, Sherman M, Deboer G, Shi W, Miyoshi E, et al. Glypican-3: a novel serum and histochemical marker for hepatocellular carcinoma. Gastroenterology 2003;125:89-97.
35. Midorikawa Y, Ishikawa S, Iwanari H, Imamura T, Sakamoto H, Miyazono K, et al. Glypican-3, overexpressed in hepatocellular carcinoma, modualates FGF2 and BMP-7 signaling. Int J Cancer 2003;103:455-465.
36. Nakatsura T, Yoshitake Y, Senju S, Monji M, Komori H, Motomura Y, et al. Glypican-3, overexpressed specifically in human hepatocellular carcinoma, is a novel tumor marker. Biochem Biophys Res Commun 2003; 306:16-25.
37. Sung YK, Hwang SY, Park YN, Farooq M, Han IS, Bae HI, et al. Glypican-3 is overexpressed in human hepatocellular carcinoma. Cancer Sci 2003;94:259-262.
38. Moriguch H, Sato C. The values and limitations of glypican-3 as a novel tumor marker for hepatocellular carcinoma from clinical and economic viewpoints. Gastroenterology 2004;127:679-680.
39. Kandil D, Leiman G, Allegretta M, Trotman W, Pantanowitz L, Goulart R, et al. Glypican-3 immunohistochemistry in liver fine-needle aspirates; a novel stain to assist in the differentiation of benign and malignant liver lesions. Cancer 2007;111:316-322.
40. Libbrecht L, Severi T, Cassiman D, Vander Borght S, Pienne J, Nevens F, et al. Glypican-3 expression distinguishes small hepatocellular carcinomas

from cirrhosis, dysplastic nodules, and focal nodular hyperplasia-like nodules. Am J Surg Pathol 2006;30:1405-1411.
41. Wang XY, Degos F, Dubois S, Tessiore S, Allegretta M, Guttmann RD, et al. Glypican-3 expression in hepatocellular tumors: diagnostic value for preneoplastic lesions and hepatocellular carcinomas. Hum Pathol 2006; 37:1435-1441.
42. Abdul-Al HM, Makhlou HR, Wang G, Goodman ZD. Glypican-3 expression in benign liver tissue with active hepatitis C: implications for the diagnosis of hepatocellular carcinoma. Hum Pathol 2008;39:209-212.
43. Nakatsuka T, Kageshita T, Ito S, Wakamatsu K, Monji M, Ikuta Y, et al. Identification of glypican-3 as a novel tumor marker for melanoma. Clin Cancer Res 2004;10:6612-6621.
44. Garrido C, Gurbuxani S, Ravagnan L, Kroemer G. Heat shock proteins: endogenous modulators of apoptotic cell death. Biochem Biophys Res Commun 2001;286:433-442.
45. Helmbrecht K, Zeise E, Rensing L. Chaperones in cell cycle regulation and mitogenic signal transduction: a review. Cell Prolif 2000;33:341-365.
46. Jolly C, Morimoto RI. Role of the heat shock response and molecular chaperones in oncogenesis and cell death. J Natl Cancer Inst 2000;92: 1564-1572.
47. Chuma M, Sakamoto M, Yamazaki K, Ohta T, Ohiki M, Asaka M, et al. Expression profiling in multistage hepatocarcinogenesis: identification of HSP70 as a molecular marker of early hepatocellular carcinoma. HEPATOLOGY 2003;37:198-207.
48. Di Tommaso L, Franchi G, Park YN, Fiamengo B, Destro A, Morenghi E, et al. Diagnostic value of HSP70, glypican 3 and glutamine synthetase in hepatocellular nodules in cirrhosis. HEPATOLOGY 2007;45:725-734.
49. Haussinger D, Sies H, Gerok W. Functional hepatocyte heterogeneity in ammonia metabolism. The intercellular glutamine cycle. J Hepatol 1985; 15:3-14.
50. Moorman AF, de Boer PA, Geerts WJ, van de Zande L, Lamers WH, Charles R. Complementary distribution of carbamoylphosphate synthetase (ammonia) and glutamine synthetase in rat liver acinus is regulated at a pretranslational level. J Histochem Cytochem 1988;36:751-755.
51. Moorman AF, Vermeulen JL, Charles R, Lamers WH. Localization of ammonia-metabolizing enzymes in human liver: ontogenesis of heterogeneity. HEPATOLOGY 1989;9:367-372.
52. Christa L, Simon MT, Flinois JP, Gebhardt R , Brechot C, Lasserre C. Overexpression of glutamine synthetase in human primary liver cancer. Gastroenterology 1994;106:1312-1320.
53. Zucman-Rossi J, Benhamouche S, Godard C, Boyault S, Grimber G, Balabaud C, et al. Differential effects of inactivated Axin1 and activated beta-catenin mutations in human hepatocellular carcinomas. Oncogene 2007;26:774-780.
54. Audard V, Grimber G, Elie C, Radenen B, Audebourg A, Letourneur F, et al. Cholestasis is a marker for hepatocellular carcinomas displaying beta-catenin mutations. J Pathol 2007;212:345-352.
55. Osada T, Sakamoto M, Nagawa H, Yamamoto J, Matsuno Y, Iwamatsu A, et al. Acquisition of glutamine synthetase expression in human hepatocarcinogenesis. Relation to disease recurrence and possible regulation by ubiquitin-dependent proteolysis. Cancer 1999;85:819-831.
56. Llovet JM, Chen Y, Wurmbach E, Roayaie S, Fiel MI, Schwarts M, et al. A molecular signature to discriminate dysplastic nodules from early hepatocellular carcinoma in HCV cirrhosis. Gastroenterology 2006;131:1758-1767.

Online Submissions: wjg.wjgnet.com
wjg@wjgnet.com
doi:10.3748/wjg.15.2296

World J Gastroenterol 2009 May 14; 15(18): 2296-2299
World Journal of Gastroenterology ISSN 1007-9327

CASE REPORT

Scirrhous hepatocellular carcinoma displaying atypical findings on imaging studies

Soo Ryang Kim, Susumu Imoto, Taisuke Nakajima, Kenji Ando, Keiji Mita, Katsumi Fukuda, Ryo Nishikawa, Yu-ichiro Koma, Toshiyuki Matsuoka, Masatoshi Kudo, Yoshitake Hayashi

Soo Ryang Kim, Susumu Imoto, Taisuke Nakajima, Kenji Ando, Keiji Mita, Katsumi Fukuda, Ryo Nishikawa, Yu-ichiro Koma, Department of Gastroenterology, Kobe Asahi Hospital, Kobe, 653-0801, Japan
Toshiyuki Matsuoka, Department of Radiology, Osaka City University Medical School, Osaka, 545-8585, Japan
Masatoshi Kudo, Department of Gastroenterology and Hepatology, Kinki University School of Medicine, Osaka-Sayama, 589-8511, Japan
Yoshitake Hayashi, Division of Molecular Medicine & Medical Genetics, International Center for Medical, Research and Treatment (ICMRT), Kobe University Graduate School of Medicine, Kobe, 650-0017, Japan
Author contributions: Kim SR, Imoto S, Nakajima T, Ando K, Mita K, and Fukuda K designed and performed the research; Matsuoka T performed the radiology research; Kudo M analyzed the data; Hayashi Y performed the pathology research; Kim SR, Nishikawa R and Koma Y wrote the paper.
Correspondence to: Soo Ryang Kim, MD, Department of Gastroenterology, Kobe Asahi Hospital, 3-5-25 Bououji-cho, Nagata-ku, Kobe, 653-0801, Japan. info@kobe-asahi-hp.com
Telephone: +81-78-6125151 Fax: +81-78-6125152
Received: November 28, 2008 Revised: April 10, 2009
Accepted: April 17, 2009
Published online: May 14, 2009

Abstract

We describe a 15-mm scirrhous hepatocellular carcinoma (HCC) in a 60-year-old man with B-type cirrhosis. Ultrasound disclosed a 15-mm hypoechoic nodule in segment 7. Contrast-enhanced US revealed heterogeneous, not diffuse, hypervascularity in the early phase and a defect in the Kupffer phase. Contrast-enhanced computed tomography (CT) revealed a heterogeneous hypervascular nodule in the early phase and a low-density area in the late phase. Magnetic resonance imaging (MRI) revealed iso- to hypointensity at T1 and high intensity at T2-weighted sequences. Contrast-enhanced MRI also revealed a heterogeneous hypervascular nodule in the early phase and washout in the late phase. Super-paramagnetic iron oxide-MRI revealed a hyperintense nodule. CT during hepatic arteriography and CT during arterial portography revealed heterogeneous hyperattenuation and a perfusion defect, respectively. Based on these imaging findings the nodule was diagnosed as a mixed well-differentiated and moderately-differentiated HCC. Histologically, the nodule was moderately-differentiated HCC characterized by typical cytological and structural atypia with dense fibrosis. Immunohistochemically, the nodule was positive for heterochromatin protein 1 and alpha-smooth muscle actin, and negative for cytokeratin 19. From the above findings, the nodule was diagnosed as scirrhous HCC. Clinicians engaged in hepatology should exercise caution with suspected scirrhous HCC when imaging studies reveal atypical findings, as shown in our case on the basis of chronic liver disease.

Key words: Scirrhous hepatocellular carcinoma; Contrast-enhanced computed tomography; Contrast-enhanced magnetic resonance imaging; Contrast-enhanced ultrasound; Computed tomography during hepatic arteriography; Computed tomography during arterial portography; Heterogeneous hypervascularity

Peer reviewers: Dr. Andreas G Schreyer, Department of Radiology, University Hospital Regensburg, Franz-Josef-Strauss-Allee 11, Regensburg 93053, Germany; Akihito Tsubota, Assistant Professor, Institute of Clinical Medicine and Research, Jikei University School of Medicine, 163-1 Kashiwashita, Kashiwa, Chiba 277-8567, Japan

Kim SR, Imoto S, Nakajima T, Ando K, Mita K, Fukuda K, Nishikawa R, Koma Y, Matsuoka T, Kudo M, Hayashi Y. Scirrhous hepatocellular carcinoma displaying atypical findings on imaging studies. *World J Gastroenterol* 2009; 15(18): 2296-2299 Available from: URL: http://www.wjgnet.com/1007-9327/15/2296.asp DOI: http://dx.doi.org/10.3748/wjg.15.2296

INTRODUCTION

According to World Health Organization (WHO) classifications, hepatocellular carcinoma (HCC) with diffuse fibrosis is subclassified as scirrhous-type HCC (SHCC)[1]. Histologically, it is characterized by diffuse fibrosis along the sinusoid-like blood spaces with varying degrees of atrophy of tumor trabeculae. Preoperative images by computed tomography (CT) and magnetic resonance imaging (MRI) are, however,

often misdiagnosed as those of cholangiolocellular carcinoma (CCC), HCC-CCC, and metastatic carcinoma due to heterogeneous enhancement in the early phase and prolonged enhancement in the late phase attributed to abundant fibrous stroma. Moreover, imaging studies for the diagnosis of SHCC, such as contrast-enhanced ultrasound (US), CT during hepatic arteriography (CTA) and CT during arterial portography (CTAP) have so far not been described. Here, we present a case of moderately differentiated SHCC that histologically manifested as typical cytological and structural atypia with dense fibrosis, whereas imaging studies with contrast-enhanced CT, MRI, US, CTA and CTAP revealed a mixed well-differentiated and moderately-differentiated HCC.

CASE REPORT

A 60-year-old man with B-type liver cirrhosis was admitted in November 2007 for further examination of a 15-mm hypoechoic nodule in segment seven (S7). The patient had no history of alcohol, blood transfusion or drug abuse. On admission, physical examination showed no remarkable abnormalities. Hepatitis B virus was positive for surface antigen and for envelope antibody, and negative for envelope antigen (HBeAg). The amount of HBV deoxyribonucleic acid was less than 2.6 log copy/mL. Laboratory studies disclosed the following abnormal values: platelets 5.3 × 10^4/μL (normal, 14-34), aspartate aminotransferase 44 IU/L (0-38), alkaline phosphokinase 864 IU/L (115-359), thymol turbidity 7.7 U (0-4), zinc sulfate turbidity test 14.8 U (2-12), and γ-globulin 29.3 g/dL (10.6-20.5). The levels of tumor markers were as follows: alpha-fetoprotein (AFP) 3.8 ng/mL (< 10), protein induced by vitamin K absence 71 mAU/mL (0-40), CA19-9 39.4 U/mL (0-37), and CEA 4.78 ng/mL (0-5).

US disclosed a 15-mm hypoechoic nodule in S7. Contrast-enhanced CT revealed a heterogeneous, not diffuse, hypervascular nodule in the early phase and a low-density area in the late phase (Figure 1A and B). MRI revealed iso- to hypointensity at T1 and high intensity at T2-weighted sequences. Contrast-enhanced MRI revealed a heterogeneous hypervascular nodule in the early phase and washout in the late phase (Figure 2A and B). Super-paramagnetic iron oxide-MRI revealed a hyperintense nodule. Contrast-enhanced US revealed heterogeneous hypervascularity in the early phase and a defect in the Kupffer phase (Figure 3A and B). CTA and CTAP revealed heterogeneous hyperattenuation and a perfusion defect, respectively (Figure 4). Based on these imaging findings, the nodule was diagnosed as a mixed well-differentiated and moderately differentiated HCC. Histologically, the nodule was moderately-differentiated HCC characterized by typical cytological and structural atypia with dense fibrosis (Figure 5A and B). Immunohistochemically, the nodule was positive for heterochromatin protein 1 and alpha-smooth muscle actin (α-SMA) (Figure 5C and D), and negative for cytokeratin 19 (CK19). From the above findings, the nodule was diagnosed as SHCC. We conducted radiofrequency ablation for the SHCC and the nodule was completely ablated. Local recurrence has not been observed over a period of 15 mo.

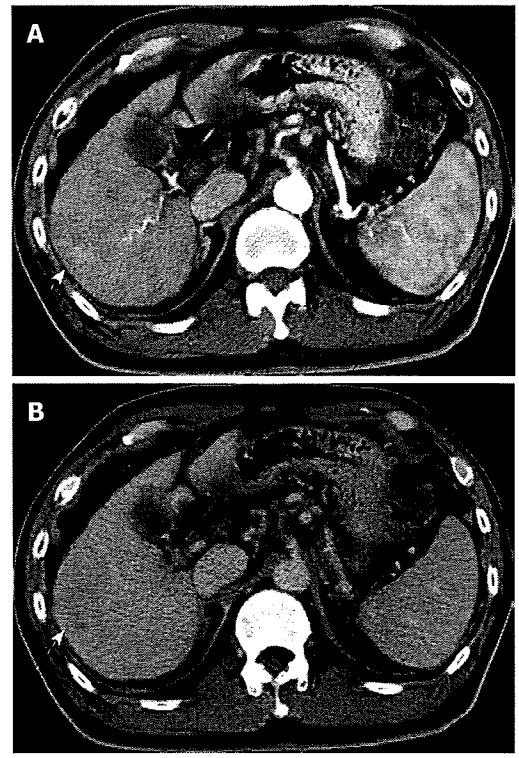

Figure 1 Contrast-enhanced CT. Heterogeneous, not diffuse, hypervascular nodule in the early phase (A) (arrow), and a low-density area in the late phase (B) (arrow).

DISCUSSION

The clinical background of SHCC is not significantly different from that of non-SHCC with regard to age, gender, positive rates to hepatitis viruses, AFP levels, Child-Pugh classification, and the stage of tumor-node-metastasis. In both morbidities, over 60% of cases are associated with chronic hepatitis rather than with liver cirrhosis. HCC patients with liver cirrhosis and liver dysfunction tend not to undergo surgery. In our case, resection was not carried out because of poor liver function attributed to liver cirrhosis.

With no clear pathological definition of SHCC, in particular a standard for the degree of the fibrosis for diagnosing the disease, its rate varies between 0.2% and 4.2%[2,3]. Regarding terminology, SHCC is often confused with "sclerosing hepatic carcinoma" that is used to designate a variety of tumors with sclerotic change and hypercalcemia arising in non-cirrhotic livers[4]. Sclerosing hepatic carcinoma does not, however, constitute a distinct histopathological entity; some of these tumors appear to be HCC, others CCC. Therefore, sclerosing hepatic carcinoma has been deleted from the WHO classification[1]. Kurogi *et al*[5] have defined SHCC as a tumor with diffuse fibrous changes in almost the entire area of the largest cross-section of the tumor and a mean fibrotic area of 39% compared with only 4.6%

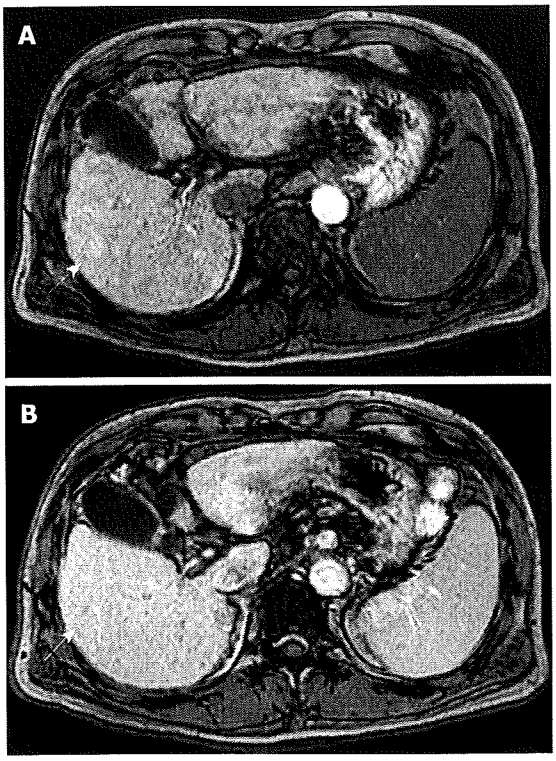

Figure 2 Contrast-enhanced MRI. A heterogeneous hypervascular nodule in the early phase (A) (arrow), and washout in the late phase (B) (arrow).

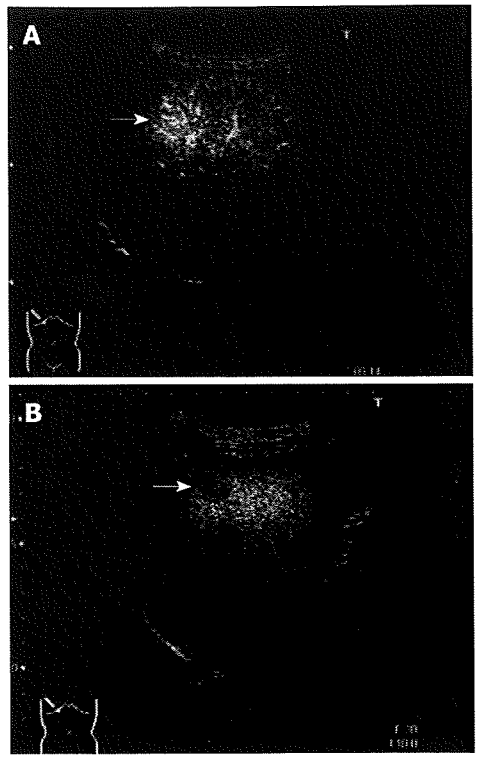

Figure 3 Contrast-enhanced US. Heterogeneous hypervascularity in the early phase (A) (arrow), and defect in the Kupffer phase (B) (arrow).

in non-SHCC.

SHCC is characterized by stellate fibrosis (84%), no encapsulation (absence of capsule) (100%), no necrosis and hemorrhage (100%), intratumoral portal tracts (80%), remarkable lymphocyte infiltration (84%), clear cell change (84%), and hyaline bodies (52%). The number of α-SMA-positive myofibroblast-like cells (activated stellate cells) in the tumor is about three times that in non-SHCC[5].

SHCC is occasionally misdiagnosed as fibrolamellar carcinoma (FLC) because of the presence of lamellar fibrosis. FLC is common in young adults and usually arises in the liver without any underlying chronic liver disease. Histologically, FLC is characterized by polyhedral, deeply eosinophilic neoplastic hepatocytes with round nuclei and distinct nucleoli, many of which contain intracytoplasmic hyaline globules and distinct pale bodies, and fibrosis arranged in a lamellar fashion around the neoplastic hepatocytes[6,7]. Conversely, although SHCC occasionally presents with lamellar fibrosis, the cancer cells being different from those of FLC, it is common in older patients with associated chronic hepatitis or liver cirrhosis[5]. Accordingly, it is not difficult to differentiate SHCC from FLC. In our case, the nodule was not diagnosed as FLC, clinically or histologically.

The US pattern was mostly hypoechoic, and contrast-enhanced CT and MRI revealed mostly heterogeneous hypervascularity in the early phase. The most characteristic feature of the imaging studies was prolonged enhancement in the late phase. Incidentally, imaging studies such as contrast-enhanced US, CTA

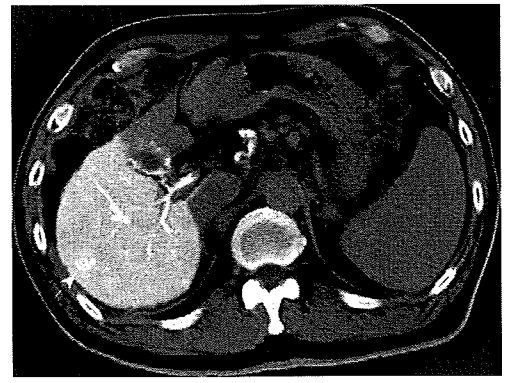

Figure 4 Heterogeneous hyperattenuation at CTA (arrow).

and CTAP have, so far, not been described for use in the diagnosis of SHCC. Misdiagnosis by imaging studies is more frequent in SHCC than non-SHCC. Of 25 cases of SHCC, nine (36%) have been diagnosed as CCC, combined HCC-CCC, and metastatic carcinoma characterized by abundant fibrous stroma, the misdiagnosis being attributed to the prolonged enhancement of the tumor in the late phase and heterogeneous enhancement in the arterial phase on contrast-enhanced CT[5].

In our case, contrast-enhanced CT, MRI, US revealed heterogeneous hypervascularity in the early phase; the nodule was not misdiagnosed as CCC or HCC-CCC because the imaging findings showed no prolonged enhancement in the late phase. The nodule was misdiagnosed as well-differentiated and moderately-

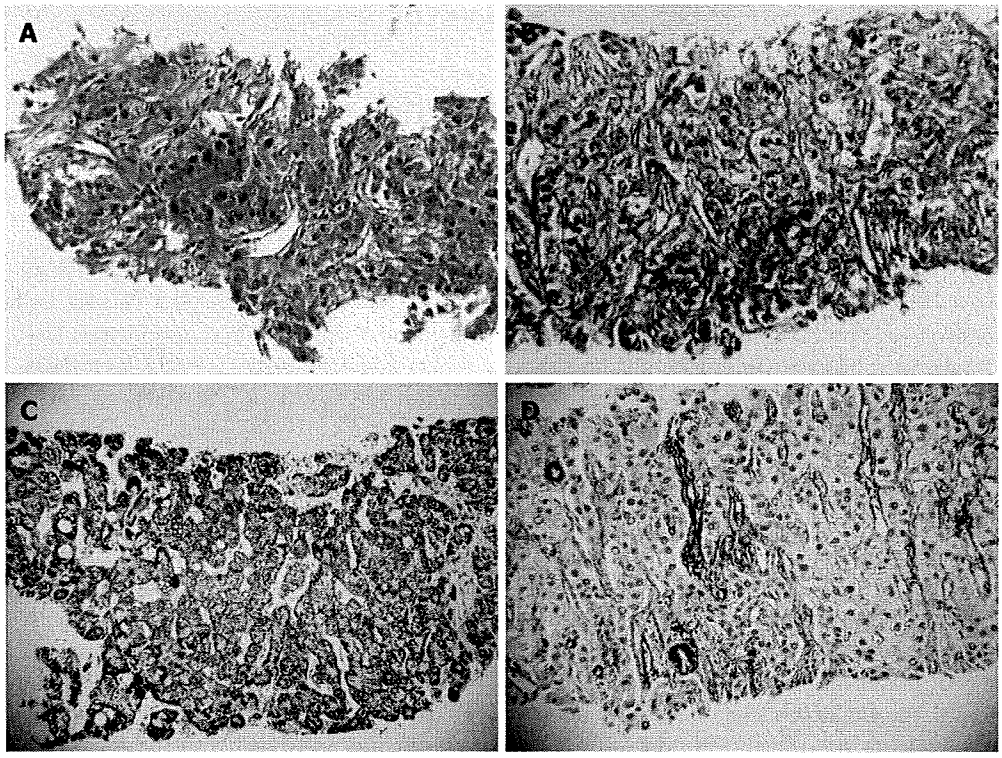

Figure 5 US-guided biopsy. Moderately-differentiated HCC characterized by typical cytological and structural atypia with dense fibrosis (HE stain) (A), (Mallory-Azan stain) (B). Positive for Hp1 (C) and α-SMA (D).

differentiated HCC on contrast-enhanced CT, MRI and US, which showed heterogeneous hypervascularity in the early phase and washout in the late phase; CTA and CTAP showed heterogeneous hypervascularity in the arterial and perfusion defect in the portal phases. Immunohistochemically, the nodule was negative for CK19 and, therefore, not CCC. Although contrast-enhanced US, CTA and CTAP did not indicate SHCC, these modalities are very effective in showing the heterogeneous vascular component, washout and perfusion defect of the nodule and contribute to precise diagnosis.

Clinicians engaged in hepatology should exercise caution with suspected SHCC when imaging studies reveal atypical findings, as shown in our case on the basis of chronic liver disease.

REFERENCES

1 **Hirohashi S**, Ishak KG, Kojiro M, Puig PL, Wanless IR, Fischer HP, Theise ND, Sakamoto M, Tsukuma H. Hepatocellular carcinoma. In: Hamilton SR, Aaltonen LA, eds. Pathology and Genetics of Tumours of the Digestive System. Lyon: IARC Press, 2000: 159-172
2 **Ishak KG**, Goodman ZD, Stocker JT. Hepatocellular carcinoma. In: Rosai J, Sobin LH, eds. Tumors of the Liver and Intrahepatic Bile Ducts, 3rd edition. Washington DC: Armed Forces Institute of Pathology, 1999: 199-230
3 **Iha H**. Clinicopathogical study on scirrhous hepatocellular carcinoma. A study of 12 resected cases. *Acta Hepatol Jpn* 1994; **28**: 855-863
4 **Omata M**, Peters RL, Tatter D. Sclerosing hepatic carcinoma: relationship to hypercalcemia. *Liver* 1981; **1**: 33-49
5 **Kurogi M**, Nakashima O, Miyaaki H, Fujimoto M, Kojiro M. Clinicopathological study of scirrhous hepatocellular carcinoma. *J Gastroenterol Hepatol* 2006; **21**: 1470-1477
6 **Craig JR**, Peters RL, Edmondson HA, Omata M. Fibrolamellar carcinoma of the liver: a tumor of adolescents and young adults with distinctive clinico-pathologic features. *Cancer* 1980; **46**: 372-379
7 **Berman MA**, Burnham JA, Sheahan DG. Fibrolamellar carcinoma of the liver: an immunohistochemical study of nineteen cases and a review of the literature. *Hum Pathol* 1988; **19**: 784-794

S- Editor Tian L **L- Editor** Stewart GJ **E- Editor** Lin YP

Journal of Viral Hepatitis, 2009, 16, 388–396 doi:10.1111/j.1365-2893.2009.01095.x

Association of genetic polymorphisms with interferon-induced haematologic adverse effects in chronic hepatitis C patients

M. Wada,[1] H. Marusawa,[1] R. Yamada,[2] A. Nasu,[1] Y. Osaki,[3] M. Kudo,[4] M. Nabeshima,[5] Y. Fukuda,[6] T. Chiba[1] and F. Matsuda[2] [1]*Department of Gastroenterology and Hepatology,* [2]*Center of Genomic Medicine, Graduate School of Medicine, Kyoto University, Kyoto, Japan;* [3]*Department of Gastroenterology and Hepatology, Osaka Red Cross Hospital, Osaka, Japan;* [4]*Department of Gastroenterology and Hepatology, Kinki University, Osaka, Japan;* [5]*Department of Gastroenterology, Nara Hospital, Kinki University, Nara, Japan; and* [6]*Department of Laboratory Science, School of Health Science, Faculty of Medicine, Kyoto University, Kyoto, Japan*

Received August 2008; accepted for publication November 2008

SUMMARY. Interferon (IFN)-based combination therapy with ribavirin has become the gold standard for the treatment of chronic hepatitis C virus infection. Haematologic toxicities, such as neutropenia, thrombocytopenia, and anaemia, however, frequently cause poor treatment tolerance, resulting in poor therapeutic efficacy. The aim of this study was to identify host genetic polymorphisms associated with the efficacy or haematologic toxicity of IFN-based combination therapy in chronic hepatitis C patients. We performed comprehensive single nucleotide polymorphism detection in all exonic regions of the 12 genes involved in the IFN signalling pathway in 32 healthy Japanese volunteers. Of 167 identified polymorphisms, 35 were genotyped and tested for an association with the efficacy or toxicity of IFN plus ribavirin therapy in 240 chronic hepatitis C patients. Multiple logistic regression analysis revealed that low viral load, viral genotypes 2 and 3, and a lower degree of liver fibrosis, but none of the genetic polymorphisms, were significantly associated with a sustained virologic response. In contrast to efficacy, multiple linear regression analyses demonstrated that two polymorphisms (*IFNAR1* 10848-A/G and *STAT2* 4757-G/T) were significantly associated with IFN-induced neutropenia ($P = 0.013$ and $P = 0.011$, respectively). Thrombocytopenia was associated with the *IRF7* 789-G/A ($P = 0.031$). In conclusion, genetic polymorphisms in IFN signalling pathway-related genes were associated with IFN-induced neutropenia and thrombocytopenia in chronic hepatitis C patients. In contrast to toxicity, the efficacy of IFN-based therapy was largely dependent on viral factors and degree of liver fibrosis.

Keywords: haematologic adverse effect, hepatitis C, interferon, single nucleotide polymorphism, sustained virologic response.

INTRODUCTION

Hepatitis C virus (HCV) infects an estimated 170 million people worldwide [1] and is a leading cause of chronic hepatitis, liver cirrhosis, and primary hepatocellular carcinoma [2]. Currently, combination therapy with ribavirin (RBV) and either conventional interferon (IFN)-α or pegylated-IFN-α (peg-IFN-α) is the gold standard of treatment for chronic HCV infection [3,4], but the overall rate of a sustained virologic response (SVR) with these therapies ranges from only 54% to 63% [5–7]. The limited therapeutic efficacy might be due to the poor virologic response in some patients or to adverse effects of the IFN-based therapy, leading to low treatment tolerance [5,6].

Predictive factors associated with a virologic response to IFN-based therapy include viral and host factors. Several studies have recently reported a possible association between the efficacy of IFN-based therapy and polymorphisms in genes encoding cytokines, chemokines, or their receptors [8–14]. The reported single nucleotide polymorphisms (SNPs) associated with a virologic response to IFN-based therapy include the *IFNAR1* [8], *IL-10* [9,10], *TNF-α* [11], *IFN-γ* [12], *CCR5* [13], *osteopontin* [14] and *TLR7* [15] genes. These data, however, are controversial and inconclusive, because most of the previous studies analysed a selected single target gene. Indeed, such limited evaluation of only one or two SNPs might not be sufficient in determining association of genetic polymorphisms with a virologic response to IFN-based therapy. Moreover, few studies have involved patients treated with combination therapy using peg-IFN-α and RBV [16,17].

Abbreviations: ALT, alanine aminotransferase; CI, confidence interval; HCV, hepatitis C virus; IFN, interferon; OR, odds ratio; PCR, polymerase chain reaction; RBV, ribavirin; SNP, single nucleotide polymorphism; SVR, sustained virologic response.

Correspondence: Hiroyuki Marusawa, MD, PhD, Department of Gastroenterology and Hepatology, Graduate School of Medicine, Kyoto University, 54 Kawahara-cho, Shogoin, Sakyo-ku, Kyoto 606-8507, Japan. E-mail: maru@kuhp.kyoto-u.ac.jp

Among the side effects of IFN plus RBV combination therapy, haematologic toxicities are frequently observed and sometimes treatment must be discontinued or the drug dose reduced, resulting in reduced efficacy of the combination therapy [5,6,18]. However, the mechanisms and predictive factors in the occurrence of these adverse effects, especially the critical decrease in blood cell count, are not clear at present.

Many studies have clarified the molecular pathway of action of IFN in detail [4,19,20]. Binding of IFN-α to its receptor induces IFNAR1 and IFNAR2 dimerization, followed by the activation of IFNAR-associated tyrosine kinases (JAK1 and TYK2). These tyrosine kinases phosphorylate STAT1 and STAT2 monomers, leading to the induction of multiple IFN-stimulated genes. Moreover, type I IFNs induce IRF7 and IRF3, which are responsible for type 1 IFN induction mediated by the virus or Toll like receptors [21]. On the other hand, the mechanisms of IFN induction in response to viral infection were recently determined [22,23]. In HCV-infected cells, the cytoplasmic RNA helicase, RIG-I, recognizes the viral dsRNA and interacts with IPS-1, leading to activation of the transcription factors, IRF3 and NF-kB, which in turn transcribe type I IFN genes. In contrast, IRF2 negatively regulates the IFN signalling pathway and recent studies suggest that IRF2 modulates the differentiation of haematopoietic cells [24–26]. Despite the unveiling of the molecular pathway of IFN signalling, it remains unclear why IFN-based therapy induces divergent efficacy or adverse haematologic toxicities in different patients.

In the present study, therefore, in order to determine the genetic factors associated with not only the efficacy but also haematologic toxicity of IFN-based therapy, we focused on the genes involved in the IFN signalling pathway, and performed a large-scale and comprehensive analysis of the genetic polymorphisms in 12 genes among chronic hepatitis C patients receiving IFN plus RBV therapy. To identify the predictors of efficacy or haematologic toxicity of IFN-based therapy, we carried out multivariate analyses using various clinicopathological factors and genetic polymorphisms.

MATERIALS AND METHODS

Patients

DNA for SNP screening was extracted from blood samples of 32 healthy Japanese volunteers under the auspices of the Pharma SNP Consortium (Tokyo, Japan). The participants comprised 240 Japanese adult chronic hepatitis C patients receiving conventional IFN-α 2b (n = 157) or peg-IFN-α 2b (n = 83) plus RBV combination therapy (Schering-Plough, Kenilworth, NJ, USA) at Kyoto University and affiliated hospitals from February 2002 to August 2007. In Japan, peg-IFN-α 2b plus RBV combination therapy was approved in October 2004. Thus, the patients who participated before and after October 2004 received conventional IFN-α 2b and peg-IFN-α 2b, respectively. Indications for IFN-based therapy included high serum values of alanine aminotransferase (ALT) and positivity for serum anti-HCV and HCV RNA. Histological examination of liver biopsy specimens was avail able for 165 (68.8%) of the 240 enrolled patients. Liver histology was assessed by an experienced hepatopathologist using the METAVIR score [27]; the fibrosis stage was defined as: F0 (no fibrosis), F1 (mild fibrosis), F2 (moderate fibrosis), F3 (severe fibrosis) and F4 (cirrhosis). The ethics committee at Kyoto University approved the studies, and informed consent for participation in the study was obtained from all patients.

IFN-α 2b or peg-IFN-α 2b plus RBV combination therapy

Patients receiving conventional IFN-α plus RBV therapy were treated with 6 million units of recombinant IFN-α 2b daily for 2 weeks and with 6 million units three times a week for the following assigned treatment period, in combination with daily oral RBV. The RBV dose was 600 mg/day in patients weighing less than 60 kg, and 800 mg/day in those weighing 60 kg or more. Patients receiving peg-IFN-α 2b plus RBV therapy were treated with peg-IFN-α 2b once per week, combined with daily oral RBV for the assigned period. The peg-IFN-α 2b dose was 1.5 μg/kg per week. Patients with genotype 1 received 48 weeks of combination therapy and patients with genotypes 2 and 3 received 24 weeks of combination therapy.

The dosage of IFN-α 2b or peg-IFN-α 2b was reduced by half if platelet counts dropped to <80 000/μL, if leucocyte counts dropped to <1500/μL, or if neutrophil counts dropped to <750/μL during therapy. IFN-α 2b or peg-IFN-α 2b was discontinued if platelet counts dropped to <50 000/μL, if leucocyte counts dropped to <1000/μL, or if neutrophil counts dropped to <500/μL during therapy. The RBV dosage was reduced to 400 mg/day or 600 mg/day if haemoglobin levels were less than 10 g/dL. RBV was discontinued if haemoglobin levels were less than 8.5 g/dL.

Sustained virologic response was defined as no detectable HCV RNA by qualitative assay for at least 24 weeks after cessation of therapy. Non-SVR was defined as no response or relapse after the cessation of therapy.

SNP screening of the IFN signalling pathway-related genes

We selected the following IFN signalling pathway-related genes, including seven genes involved in the intracellular IFN-mediated signalling pathway from the binding of IFN to its receptor to initiation of the transcription of various target genes [20]; four genes involved in the RIG-I signalling pathway, which triggers the IFN-induction pathway after viral infection [22,23], and one gene that negatively regulates the IFN signalling pathway [24] [IFNAR1 (NT_011512.10, NM_000629.2), IFNAR2 (NT_011512.10, NM_207585.1), JAK1 (NT_032977.7, NM_002227.1), TYK2 (NT_011295.10, NM_003331.3), STAT1 (NT_005403.15, NM_007315.2), STAT2 (NT_029419.10, NM_005419.2), IRF9 (NT_026437.11, NM_006084.3), RIG-I (NT_

008413.16, NM_014314.2), IPS-1 (NT_011387.8, NM_020746.1), IRF3 (NT_011109.15, NM_001571.2), IRF7 (NT_035113.6, NM_004031.1), and IRF2 (NT_0022792.17, NM_002199.3)]. Genomic DNA was extracted from blood samples of 32 healthy Japanese volunteers using a DNA extraction kit (Genomix Kit; TALENT, Trieste, Italy), and the 179 exons, including the 5′- and 3′-untranslated regions and adjacent intronic regions of the 12 candidate genes, were amplified. The resultant polymerase chain reaction (PCR) products were used as templates for direct sequencing on an ABI 3730 automated sequencer (Applied Biosystems, Foster City, CA, USA). Segregating sites were identified and genotypes were confirmed directly from electrophorograms using Genalys (http://www.software.cng.fr/docs/genalys.html) [28].

SNP genotyping

Among the SNPs identified by the screening, we selected tag SNP markers that covered all of the common (>5% frequency) haplotypes using the minimal haplotype tagging method, one of the best methods to identify the smallest tagging set for an arbitrary region of the genome [29]. These tag SNPs allowed us to genotype the smallest possible number of SNPs for each gene while resolving all common haplotypes. We also included SNPs that existed in coding sequences or 5′ flanking regions with frequencies higher than 5%. These SNPs were genotyped using the ABI Taqman allelic discrimination method and an ABI 7900HT sequence detection system (Applied Biosystems). Primers and probes were designed by the manufacturer with SNP browser Software (Applied Biosystems), as shown in Tables S1 and S2. Amplification reactions were performed in a 3 μL volume, with 5 ng DNA, 1.5 μL universal PCR master-mix, and 0.0375 μL assay mix with the specific primers and probes. Seven SNPs that could not be detected using the Taqman assay were determined by direct sequencing of PCR products amplified with primers specific for each SNP (Table S3).

Statistical analysis

Genotype distributions were tested for Hardy–Weinberg equilibrium using exact tests. To identify predictors of SVR, we used univariate analysis of pre-treatment factors to compare all SVR and non-SVR patients who had completed the treatment. The following pre-treatment factors were considered: SNPs, sex (male *vs* female), age (in years), weight (in kilograms), serum ALT, IFN history (naive *vs* relapse *vs* nonresponse), HCV genotype (1 *vs* 2 and 3), HCV viral load (<100 *vs* 100 to <500 *vs* 500 to <850 *vs* ≥850 kIU/mL), and fibrosis stage (F0 *vs* F1 *vs* F3 *vs* F4). Allele and genotype frequencies were evaluated for their association with SVR using Fisher's exact tests. Sex, IFN history, and HCV genotype were evaluated using the chi-square test. Age, weight, and serum ALT were evaluated using the Mann–Whitney *U*-test. Fibrosis stage and viral load were evaluated using a trend chi-square test. We considered two-tailed *P*-values <0.05 to be statistically significant and calculated odds ratios (ORs) and 95% confidence intervals. Multiple logistic regression analysis was performed using STATISTICA (StatSoft, Tulsa, OK, USA) to evaluate the association between SVR and significant factors from the univariate analyses.

To identify predictors of cytopenia, we examined the association between decreased leucocyte, neutrophil, and platelet counts and haemoglobin levels, and the following patient characteristics and clinical features using linear regression analysis with STATISTICA: sex, age, weight, fibrosis stage and SNPs. Multiple linear regression analysis was performed to evaluate the association between the decreased peripheral blood cell numbers and significant factors from the univariate analyses.

RESULTS

Genetic variations and polymorphisms in IFN signalling pathway-related genes

By screening 32 healthy volunteers, we identified 167 genetic polymorphisms (153 SNPs and 14 insertions/deletions) in the 12 IFN signalling pathway-related genes (Table 1, Table S4). All identified polymorphisms were in Hardy–Weinberg equilibrium. Of these 167 polymorphisms, 60 (49 SNPs and 11 insertions/deletions) were novel and were not registered in Build 125 of the SNP database (http://www.ncbi.nlm.nih.gov) (Table 2). Among the 167 SNPs identified, 30 (16 nonsynonymous and 14 synonymous) were located in exons and we confirmed that 14 of the 30 SNPs identified in the exons were novel. Furthermore, we identified 10 novel nonsynonymous variants in the seven genes. Sixty-two SNPs were relatively uncommon (minor allele frequency <0.05) and were thus excluded from further analysis. Finally, 27 selected tag SNPs and eight additional SNPs that existed in coding sequences or 5′ flanking regions were subjected to further genotyping analyses in chronic hepatitis C patients (Table 2).

Variables associated with virologic response to IFN-based therapy

The relationship between baseline characteristics and virologic response to the IFN plus RBV combination therapy in chronic hepatitis C patients is summarized in Table 3. Combination therapy was discontinued in 37 patients during the assigned treatment period. These 37 patients were excluded from analysis of the virologic response. SVR was achieved in 98 of 203 (48.3%) patients, and 105 patients (51.7%) had a relapse of HCV infection after the end of therapy or showed no response to IFN-based therapy.

To determine the predictive factors for IFN-based therapy efficacy, we examined the correlation between virologic response, and clinical and viral factors. Of 56 patients with